Formulation of PEG–folic acid coated nanometric DNA particles from perfluoroalkylated cationic dimerizable detergents and *in vitro* folate-targeted intracellular delivery

Loïc Le Gourriérec, Christophe Di Giorgio, Jacques Greiner and Pierre Vierling*

Received (in Montpellier, France) 10th April 2008, Accepted 8th May 2008
First published as an Advance Article on the web 17th July 2008
DOI: 10.1039/b806043f

Present attempts in gene delivery mediated with synthetic vectors are now oriented towards the formulation of nanometric DNA complexes reminiscent of viruses. The assembly of such multifunctional gene transfer systems was designed in order to take advantages of viral vector properties. This requires, among others, the formulation of very small- and homogeneously-sized "stealth" as well as ligand-labeled DNA nanoparticles. In this paper, we report the straightforward synthesis of an original dimerizable perfluoroalkylated thiol detergent deriving from cysteine and containing a monocationic aminotriethylene glycol and of a known analog containing a tricationic linear spermine polar head (three steps, 45–50% overall yields). These derivatives condensed DNA into a monodisperse population of negatively or positively charged, virus-sized ($\sim$40–80 nm) [F-detergent]$_2$/DNA nanoparticles, as confirmed by zeta potential and agarose gel electrophoresis experiments. These stable nanoparticles consisted likely of monomolecular DNA particles although particles containing a very few copies of DNA could not be excluded. These constructs were obtained following a monomolecular DNA condensation process occurring when DNA is mixed with a cationic detergent at a concentration close to its critical micellar concentration, the resulting complexes being subsequently stabilized upon oxidation of the thiol detergent into its disulfide lipidic dimer ([F-detergent]$_2$) on the DNA matrix. DNA was also shown to be fully protected, not accessible, when condensed into cationic nanoparticles. The surface of these particles was further labeled with an amphiphilic-polyethyleneglycol–folic acid conjugate, as attested by zeta potential measurements. Size measurements and TEM analysis showed nanometric sizes ($\leq$100 nm) for these labeled DNA nanoparticles. Noticeably with respect to their very low size, we found that the cationic, uncoated [F-detergent]$_2$/DNA formulations were efficient "non-specific" transfection agents of KB cells and particularly more efficient than PEI polyplexes. However, though FACS analysis with (un)coated and YOYO-labeled [F-detergent]$_2$/DNA nanoparticles showed specific uptake of the folic acid coated nanoparticles into folate-overexpressing KB cells, transfection experiments relying on luciferase expression measurements did not show any specific improvement of gene expression resulting from such a targeting.

Introduction

Present attempts in gene delivery mediated with synthetic vectors are now oriented towards the formulation of nanometric DNA complexes reminiscent of viruses (*e.g.* "artificial" or "synthetic" viruses).[1–6] The assembly of such multifunctional gene transfer systems was designed in order to take advantages of viral vectors properties such as their small size ($\leq$100 nm), capability to escape the immune system sentinels, cell tropism, cytoplasm delivery and/or nuclear targeting and penetration.[1,2,4,5,7] This requires, among others, the formulation of very small- and homogeneously-sized "stealth" as well as ligand-labeled DNA nanoparticles. A small particle size is indeed considered to be critical for facilitating diffusion—extravasation through blood vessels,[8] diffusion through mucus,[9,10] cytoplasm,[11,12] nuclear pores (which block translocation of macromolecules larger than 39 nm in diameter)[13]—or ligand–receptor mediated cellular uptake,[14,15] as well as for benefiting from the enhanced permeation effect (passive accumulation within the tumor mass).[16] Formulation of very small-sized DNA nanoparticles can be achieved in a highly controllable and reproducible fashion by a "monomolecular DNA condensation" process.

This could be achieved with dimerizable cationic detergents[17–20] such as the thiols shown in Fig. 1, which were developed by Behr's group.[17–19] DNA condensation with these cationic detergents ensures monodispersity, owing to reversible DNA/detergent and detergent/micelle interactions, and the largest number of DNA particles, each particle being ultimately made of a single molecule or copy of condensed DNA, owing to entropy.[21,22]

Once the monomolecular detergent/DNA nanoparticles had formed with the dimerizable cationic thiol detergents, the

Laboratoire de Chimie des Molécules Bioactives et des Arômes, UMR 6001, Université de Nice Sophia-Antipolis, CNRS, Institut de Chimie de Nice, 28, avenue de Valrose, 06108 Nice Cédex 2, France. E-mail: vierling@unice.fr; Fax: 33(0)49207651; Tel: 33(0)492076143

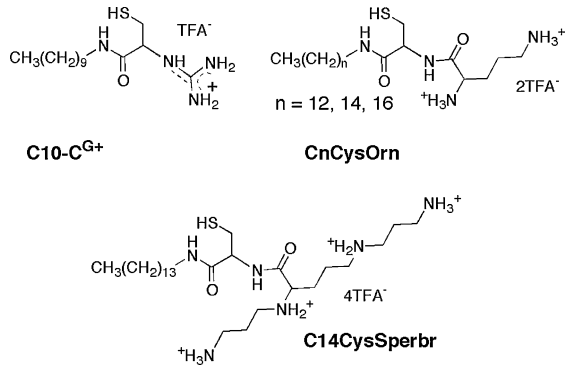

Fig. 1 Hydrocarbon cationic dimerizable thiol detergents for complexation of DNA reported in literature.[17–19]

particles were then stabilized by oxidation of the thiol detergents into disulfide lipids (noted $[detergent]_2$) on the DNA matrix.[17–19] This particular phenomenon led to $[detergent]_2$/DNA nanoparticles with a negative zeta potential, but wherein DNA is exposed to degradation, and which suffered from a lack of *in vitro* transfection properties.[17–19] This was reported to be likely due to their negative surface charge, which would not allow any attractive electrostatic interactions with the anionic proteoglycan proteins expressed on the cell surface and, consequently, to an inefficient cell binding and internalization.

Based on Behr's group results and on a "monomolecular DNA condensation" process, our group explored the development of stable monomolecular DNA, but cationic nanoparticles, wherein DNA is fully protected, and which should be able to display efficient cell transfection properties, as a result of increased contact to the anionic cell surface and internalization by endocytosis. Our group succeeded in obtaining such cationic DNA nanoparticles from the perfluoroalkylated dimerizable detergents (denoted F-detergent) containing the linear tricationic (*i.e.* N-F4C10CysSperlin) or branched tetracationic (*i.e.* F4C11CysSperbr) spermine polar head shown in Fig. 2.[23]

Actually, the challenge was to design dimerizable polycationic detergents that display a critical micellar concentration (CMC) high enough for the monomer to perform monomolecular DNA condensation and low enough for its dimer to form stable nanoparticles capable of efficient cell transfection. It should be noted that only mono- and di-amino dimerizable detergents led to monomolecular DNA nanoparticles. Polycationic ones remained unsuccessful because of their too high hydrophilicity, even after their dimerization into lipids, which did not allow stable complexation with the DNA matrix.[18,19] Thus, to counterbalance the hydrophilic character of a polycationic polar head and to increase the hydrophobic character of the resulting detergent, we selected highly fluorinated hydrophobic chains for their ability to increase hydrophobic interactions and to promote self-aggregation of the amphiphiles, and, consequently, to decrease the CMC with respect to their hydrocarbon counterparts.[24–26] Unfortunately, the monomolecular cationic $[F\text{-detergent}]_2$/DNA nanoparticles were, *in vitro*, also poor transfection systems.[23] These results were attributed to the very small size of these nanocomplexes, which, owing to Brownian motion, prevents them from sedimentation and adsorption onto the adherent cell monolayer and, consequently, from proteoglycan-triggered endocytosis. Nevertheless, and with respect to their very small size (*e.g.* $\leq$40 nm) and poor transfection efficiency as a non-specific gene transfer system, which is governed by electrostatic interactions, the $[F\text{-detergent}]_2$/DNA nanoparticles constitute an ideal matrix for the building-up of synthetic viruses. Moreover, one could also benefit from the unique properties that have been evidenced for "fluorinated" lipoplexes in terms of stability in biological fluids and improved *in vitro* and *in vivo* transfection potential.[26,27]

The next steps of this work consisted (i) in extending the collection of perfluoroalkylated cationic and dimerizable detergents forming stable cationic monomolecular DNA nanoparticles, and (ii) in labeling the resulting nanoparticles with elements increasing their blood circulation time and cell recognition in order to favor specific receptor-mediated endocytosis. Aiming at the former goal, we selected the new N-F4C10CysTEGNH3 detergent shown in Fig. 2 for its monocationic aminotriethylene glycol polar head, which should be to some extent less hydrophilic than the linear (tricationic) or branched (tetracationic) spermine analogs shown in Fig. 2. For the labeling of the monomolecular DNA nanoparticles, we selected the perfluoroalkylated amphiphilic PEG–folic acid conjugate[28] shown in Fig. 2, which, by hydrophobic/fluorophilic anchorage into the micellar domains of the $[F\text{-detergent}]_2$/DNA nanoparticles, will provide a PEG-folic acid envelope covering these particles. Extended blood circulation times and cancer cell recognition could therefore be achieved with PEG and folic acid, respectively. We have chosen folic acid not only as a targeting ligand because numerous fast dividing cancer cells over-express a high affinity folic acid receptor[16,29–38] but also as a model to validate our approach.

In this paper, we report on (i) the preparation of the new perfluoroalkylated, monocationic dimerizable detergent N-F4C10CysTEGNH3 shown in Fig. 2, (ii) an improved synthesis of the tricationic N-F4C10CysSperlin detergent (which was initially obtained with only 7% yield using a five-step procedure[23]), (iii) the detailed physico-chemical analysis of the ability of the N-F4C10CysTEGNH3, N-F4C10CysSperlin and F4C11CysSperbr detergents to condense DNA into negatively and positively charged nanometric $[F\text{-detergent}]_2$/DNA particles, (iv) the surface modification of these nanoparticles with the perfluoroalkylated amphiphilic-PEG–folic acid conjugate[28] shown in Fig. 2, and (v) the *in vitro* specific cell uptake and transfection of folate-overexpressing cells with these PEG-folic acid-labeled systems.

Experimental

General experimental and analytical conditions

All the reactions were performed in anhydrous solvents under dry and oxygen-free nitrogen. Anhydrous solvents were prepared by standard methods. Column chromatographies were performed on Merck silica gel 60 (mesh 70–230). Reactions were monitored by thin-layer chromatography (TLC)

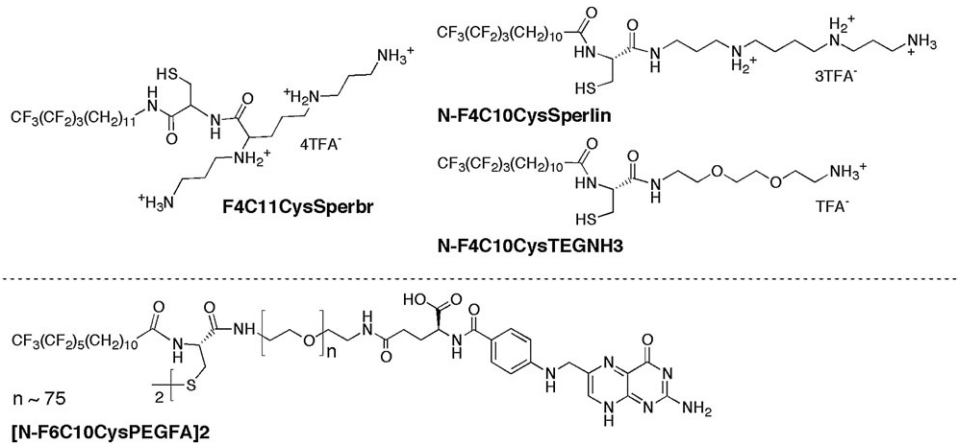

Fig. 2 Perfluoroalkylated cationic dimerizable thiol detergents for monomolecular condensation of DNA (top) and amphiphilic-PEG–folate targeting conjugate[28] for post-labeling (bottom). Compounds N-F4C10CysSper and F411CysSperbr are described in ref. 23. The new detergent N-F4C10CysTEGNH3 is described in this work.

using silica plates (SDS $60F_{254}$), visualized by UV light (254 nm) and by spraying with ninhydrin reagent (Sigma) or with 5,5′-dithiobis(2-nitrobenzoic acid) (DTNB) (Sigma), or by charring with H_2SO_4. 1-(3-Dimethylaminopropyl)-3-ethylcarbodiimide hydrochloride (EDC), 4-(dimethylamino)pyridine (DMAP), hydroxybenzotriazole (HOBt), triethylamine, and trifluoroacetic acid (TFA) were purchased from Sigma, oxalyl chloride from Fluka, 1,1-dimethylethyl *N*-[2-[2-(2-aminoethoxy)ethoxy]ethyl]carbamic acid, **5**, from IRIS Biotech. These chemicals were used as received. 11-Perfluorobutylundecanoic acid,[39] dimethylthiazolidine-4(*R*)-carboxylic acid (hydrochloride salt), **1**,[40] *N*,*N*′,*N*″-triBoc-spermine, **6**,[41] F4C11CysSperbr,[23] and $[N\text{-}F6C10CysPEGFA]_2$ conjugate[28] were prepared following literature procedure.

^1H, ^{13}C and ^{19}F NMR spectra were recorded on a Bruker AC 200 (or AC 500) spectrometer at 200 (or 500), 50.3 (or 125.8) and 188.3 MHz, respectively. Chemical shifts (δ) were measured relative to $CDCl_3$ (7.26 ppm) or DMSO-d_6 (2.50 ppm) for ^1H, to that of $CDCl_3$ (76.9 ppm) or DMSO-d_6 (39.5 ppm) for ^{13}C, and to that of $CFCl_3$ (0 ppm) for ^{19}F. In the ^{13}C NMR data, the carbon atoms attached to fluorine atoms were omitted, due to extensive couplings. The following abbreviations were used to describe the signal multiplicities: s (singlet), bs (broad singlet), d (doublet), t (triplet), and m (multiplet). Chemical shifts were expressed in parts per million (ppm), coupling constants (J) were reported in hertz, and signals were listed as follows: shifts in ppm (multiplicity, coupling, integration and assignment). COSY $^1H/^1H$, $^1H/^{13}C$ NMR correlation (on Bruker AC 500 spectrometer), and/or mass spectrometry data fully confirm the signal assignments and structure of the isolated materials. Electrospray ionization mass spectrometry (ESI-MS) in positive and negative mode was performed on a Bruker Daltonics (Esquire 3000 plus) apparatus equipped with atmospheric pressure ionization (API) source.

Synthesis of N-F4C10CysTEGNH3 (Scheme 1)

3-(12,12,13,13,14,14,15,15,15-Nonafluoropentadecanoyl)-2,2-dimethyl-4(*R*)-thiazolidine-4-carboxylic acid, 2. Oxalyl chloride (195 μL, 2.25 mmol) and DMF (10 μL) were successively added to 11-perfluorobutylundecanoic acid (600 mg, 1.5 mmol) dissolved in CH_2Cl_2 (20 mL). After the sample was stirred overnight at room temperature, the solvent was removed under vacuum. The crude acid chloride dissolved in anhydrous CH_2Cl_2 (2.5 mL) was added dropwise to a CH_2Cl_2 solution (20 mL) containing compound **1** (360 mg, 2.25 mmol) and triethylamine (0.6 mL). The reaction mixture was stirred at room temperature for 3 h. The reaction mixture was washed with an aqueous 0.2 N $KHSO_4$ solution, then dried over Na_2SO_4, filtered, and concentrated. The residue was purified by chromatography over silica gel (100 : 0 to 96 : 4 CH_2Cl_2–MeOH) to yield compound **2** as a white powder (735 mg, 70%). R_f 0.40 (9 : 1 CH_2Cl_2–MeOH). ^1H NMR ($CDCl_3$, 200 MHz): δ 8.09 (br s, 1H, C(O)OH), 4.85 (t, J 3.7 Hz, 1H, CHC(O)O), 3.32 (m, 2H, CH_2S), 2.22 (t, J 7.2 Hz, 2H, $CH_2C(O)$), 2.08 (m, 2H, CF_2CH_2), 1.89 and 1.83 (2s, 6H, CH_3), 1.45–1.70 (m, 4H, $CF_2CH_2CH_2$ and $CH_2CH_2C(O)$), 1.27 (br s, 12H, $(CH_2)_6CH_2CH_2C(O)$). ^{13}C NMR ($CDCl_3$, 50.3 MHz): δ 174.87 (C(O)OH), 171.86 (C(O)N), 73.86 (CH_3C), 65.76 ($CHC(O)O$), 36.93 ($CH_2C(O)$), 31.43 (CH_2S), 30.90 (t, J_{CF} 22.3 Hz, CF_2CH_2), 29.83 and 27.66 (CH_3), 29.22, 29.35, 29.48, 29.53, and 29.62 ($(CH_2)_6CH_2CH_2C(O)$), 25.09 ($CH_2CH_2C(O)$), 20.19 (t, J_{CF} 3.7 Hz, $CF_2CH_2CH_2$). ^{19}F NMR ($CDCl_3$, 188.3 MHz): δ −81.58 (3F, CF_3), −115.21 (2F, CF_2CH_2), −125.04 (2F, $CF_3CF_2CF_2$), −126.61 (2F, CF_3CF_2). ESI-MS (negative mode): $(M + CF_3CO_2)^-$ = 660.2; $(M - H)^-$ = 546.2 in agreement with the mass calculated for M = $C_{21}H_{30}F_9NO_3S$ (547.18).

***N*-[8-[[(1,1-Dimethylethoxy)carbonyl]amino]-3,6-dioxaoctyl]-3-(12,12,13,13,14,14,15,15,15-nonafluoropentadecanoyl)-2,2-dimethyl-(4*R*)-thiazolidine-4-carboxamide, 3.** Compound **2** (203 mg, 0.42 mmol) was added to a solution of **5** (220 mg, 0.85 mmol), HOBt (110 mg, 0.85 mmol), EDC (156 mg, 0.8 mmol) and DMAP (50 mg, 0.4 mmol) in anhydrous DMF (20 mL). The reaction was stirred for 4 h at room temperature until complete disappearance of **2** (TLC monitoring 90 : 10 CH_2Cl_2–MeOH, $KMnO_4$). DMF was removed under vacuum, the colourless oil dissolved in CH_2Cl_2 was washed with aq. 0.4 M $KHSO_4$ solution, then dried over Na_2SO_4 and concentrated. Purification was performed over

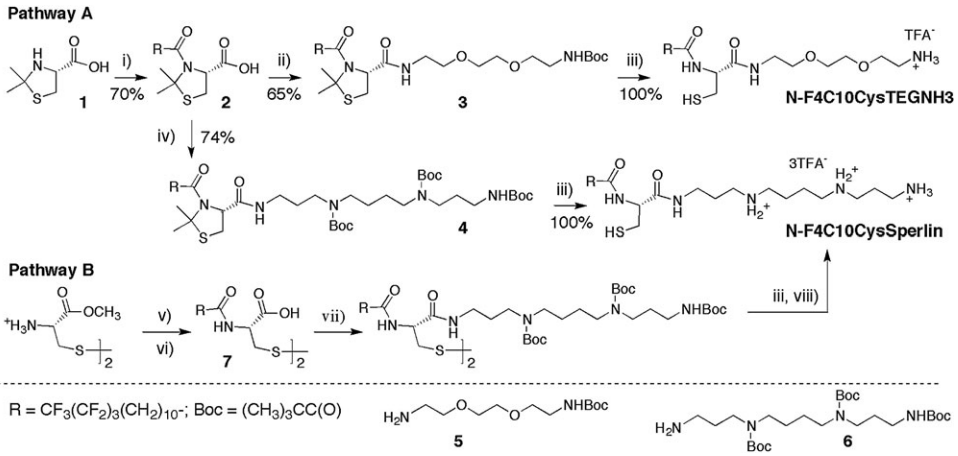

Scheme 1 Synthesis of the perfluoroalkylated thiol N-F4C10CysTEGNH3 and N-F4C10CysSperlin detergents. *Reagents and conditions*: (i) $CF_3(CF_2)_3(CH_2)_{10}C(O)Cl$ [prepared *in situ* from acid and $(COCl)_2$], Et_3N, CH_2Cl_2; (ii) HOBt, EDC, DMAP, **5**, rt, DMF; (iii) TFA, CH_2Cl_2; (iv) HOBt, EDC, DMAP, **6**, rt, DMF; (v) $CF_3(CF_2)_3(CH_2)_{10}C(O)OH$, BOP, HOBt, Et_3N, DMF; (vi) 2N HCl in dioxane; (vii) BOP, HOBt, **6**, Et_3N, CH_2Cl_2; (viii) Zn, AcOH.

silica gel chromatography (80 : 20 CH_2Cl_2–cyclohexane to 98 : 2 CH_2Cl_2-MeOH) to afford **3** as a white solid (195 mg, 65%). R_f 0.52 (96 : 4 CH_2Cl_2–MeOH). ^{1}H NMR ($CDCl_3$, 200 MHz): δ 6.64 (m, 1H, CHC(O)N*H*CH_2), 5.10 (t, *J* 5.0 Hz, 1H, NHC(O)O), 4.66 (d, *J* 5.6 Hz, 1H, C(O)NCH), 3.62–3.42 (m, 10H, NHCH_2CH_2O and OCH_2), 3.32–3.15 (m, 4H, CH_2S and CH_2NHBoc), 2.28–1.86 (m, 4H, CF_2CH_2 and $CH_2C(O)$), 1.94 and 1.79 (2s, 6H, $(CH_3)_2C$), 1.66–1.48 (m, 4H, $CF_2CH_2CH_2$ and C$H_2$$CH_2C(O)$), 1.40 (s, 9H, $(CH_3)_3C$), 1.24 (br s, 12H, $(CH_2)_6CH_2CH_2C(O)$). ^{13}C NMR ($CDCl_3$, 50.3 MHz): δ 171.68 (C(O)N), 170.50 (C(O)NH), 155.93 (NHC(O)O), 79.12 ($(CH_3)_3C$), 73.81 ($(CH_3)_2C$), 70.37, 70.28, 70.11 and 69.52 (CH_2O), 67.30 (C(O)N*C*H), 40.29 (*C*H_2NHC(O)O), 39.41 (CHC(O)NH*C*H_2), 36.77 (*C*$H_2C(O)$), 32.03 (CH_2S), 30.69 (t, *J* 22.4 Hz, CF_2CH_2), 29.32, 29.24, 29.21, 29.09 and 28.87 ($(CH_2)_6CH_2CH_2C(O)$ and $(CH_3)_2C$), 28.31 ($(CH_3)_3C$), 24.78 ($CH_2CH_2C(O)$), 19.96 (t, *J* 3.7 Hz, $CF_2CH_2CH_2$). ^{19}F NMR ($CDCl_3$, 188.3 MHz): δ −81.59 (3F, CF_3), −115.11 (2F, CF_2CH_2), −125.02 (2F, $CF_3CF_2CF_2$), −126.58 (2F, CF_3CF_2).

***N*-[(1*R*)-1-(Mercaptomethyl)-2-oxo-2-(8-amino-3,6-dioxaoctylamino)ethyl]-12,12,13,13,14,14,15,15,15-nonafluoropentadecanamide, N-F4C10CysTEGNH3.** Full deprotection (Boc and thiazolidine ring) was achieved by stirring **3** (115 mg, 0.165 mmol) at room temperature in a 1 : 1 CH_2Cl_2–TFA solution for 4 h to afford quantitatively compound N-F4C10CysTEGNH3 (monoTFA salt) as a white solid (112 mg, 100%) stored under argon atmosphere. R_f 0.42 (92 : 8 CH_2Cl_2–MeOH); ^{1}H NMR (C_2D_5OD, 500 MHz): δ 4.48 (t, *J* 6.5 Hz, 1H, C(O)NHC*H*), 3.76 (t, *J* 5.0 Hz, 2H, $CH_2CH_2NH_3^+$), 3.70–3.64 (m, 4H, OCH_2), ~3.57 ($C(O)NHCH_2CH_2$ hindered by residual non-deuterated EtOD, determined by HSQC), 3.46 and 3.39 (2td, J_{AB} 14.0, J_{BX} = J_{AX} 5.5 Hz, 1H, C(O)NHC$H_{2(A,B)}$), 3.15 (t, *J* 4.9 Hz, 2H, $CH_2NH_3^+$), 2.90 (dd, J_{AB} 13.7, J_{AX} 5.8 Hz, 1H, CH_AH_BSH), 2.80 (dd, J_{AB} 13.7, J_{BX} 7.2 Hz, 1H, CH_AH_BSH), 2.31 and 2.30 (2t, J 7.5 Hz, 2H, $CH_2C(O)$), 2.14 (tt, J_{HF} 19.0, J_{HH} 8.5 Hz, 2H, CF_2CH_2), 1.70–1.60 (m, 4H, $CF_2CH_2CH_2$ and C$H_2$$CH_2C(O)$), 1.48–1.31 (m, 12H, $(CH_2)_6CH_2CH_2C(O)$). ^{13}C NMR (C_2D_5OD, 125.8 MHz): δ 175.03 ($CH_2C(O)$), 171.46 (CH*C*(O)NH), 70.44 (O*C*H_2), 69.57 (C(O)NHCH_2*C*H_2), 66.99 (*C*$H_2CH_2NH_3^+$), 56.76 (*C*HC(O)NH), 39.68 (*C*$H_2NH_3^+$), 39.33 (C(O)NH*C*H_2), 35.95 (*C*$H_2C(O)$), 30.83 (t, *J* 22.3 Hz, CF_2CH_2), 29.62, 29.53, 29.46, 29.38, and 29.22 ($(CH_2)_6CH_2CH_2C(O)$), 25.96 (*C*$H_2CH_2C(O)$ and CH_2SH), 20.35 (t, *J* 3.7 Hz, $CF_2CH_2CH_2$). ^{19}F NMR (C_2D_5OD, 188.3 MHz): δ −75.53 (3F, CF_3COO^-), −82.70 (3F, CF_3), −115.82 (2F, CF_2CH_2), −125.68 (2F, $CF_3CF_2CF_2$), −127.43 (2F, CF_3CF_2). ESI-MS (positive mode): $(M + H)^+$ = 638.3 in agreement with the mass calculated for M = $C_{24}H_{40}F_9N_3O_4S$ (637.26).

Synthesis of N-F4C10CysSperlin (Scheme 1)

***N*-[4,9,13-Tris[(1,1-dimethylethoxy)carbonyl]-4,9,13-triazatridecyl]-3-(12,12,13,13,14,14,15,15,15-nonafluoropentadecanoyl)-2,2-dimethyl-(4*R*)-4-thiazolidinecarboxamide, 4.** Compound **2** (50 mg, 0.09 mmol) was added to a solution of **6** (60 mg, 0.12 mmol), HOBt (16 mg, 0.12 mmol), EDC (25 mg, 0.12 mmol) and DMAP (4.5 mg, 0.036 mmol) in anhydrous DMF (5 mL). The reaction was stirred for 4 h at room temperature until complete consumption of **2** (TLC monitoring 90 : 10 CH_2Cl_2–MeOH, $KMnO_4$). DMF was removed under vacuum, the crude oil dissolved in CH_2Cl_2 was washed with aq. 0.4 N $KHSO_4$ solution, then dried over Na_2SO_4 and concentrated. Purification was performed over silica gel chromatography (80 : 20 CH_2Cl_2–cyclohexane to 95 : 5 CH_2Cl_2–MeOH) to afford **4** as a colourless oil (70 mg, 74%). ^{1}H-NMR ($CDCl_3$, 200 MHz): δ 7.63 (br s, 1H, CHC(O)N*H*), 5.38 (br s, 1H, NHC(O)O), 4.64 (br d, *J* 5.8 Hz, 1H, C*H*C(O)NH), 2.95–3.45 (m, 14H, NCH_2 and CH_2S) 2.25–1.85 (m, 4H, $CH_2C(O)$ and CF_2CH_2), 2.03 and 1.80 (2s, 6H, $(CH_3)_2C$), 1.75–1.50 (m, 12H, CH_2CH_2N, C$H_2CH_2C(O)$ and $CF_2CH_2CH_2$), 1.43, 1.41, and 1.40 (each s, each 9H, $(CH_3)_3C$), 1.24 (br s, 12H, $(CH_2)_6CH_2CH_2C(O)$); ^{19}F NMR ($CDCl_3$, 188.3 MHz): δ −81.51 (3F, CF_3), −115.14 (2F, CF_2CH_2), −125.00 (2F, $CF_3CF_2CF_2$), −126.56 (2F, CF_3CF_2).

***N*-[(1*R*)-1-(Mercaptomethyl)-2-oxo-2-(4,9,13-triazatridecylamino)ethyl]-12,12,13,13,14,14,15,15,15-nonafluoropentadecanamide, N-F4C10CysSperlin.** The full deprotection (Boc and thiazolidine ring) was achieved by stirring **4** (70 mg, 0.07 mmol) at room temperature in a 1 : 1 CH_2Cl_2–TFA solution for 4 h to afford quantitatively compound N-F4C10CysSperlin (as its triTFA salt) as a white solid (72.4 mg, 100%) stored under an argon atmosphere. ^{1}H NMR (C_2D_5OD, 500 MHz): δ 4.40 (t, J 6.5 Hz, 1H, C(O)NHC*H*), 3.43 (t, J 6.7 Hz, 1.4H, C(O)NHCH_2) and 3.39 (t, J 5.7 Hz, 0.6H, C(O)NHC*H*), 3.20 (t, J 7.5 Hz, 2H, C(O)NHCH$_2$CH$_2$CH_2), 3.15–3.04 (m, 8H, CH_2N$^+$), 2.89 (dd, J_{AB} 14.0, J_{AX} 6.0 Hz, 1H, CH_AH$_B$SH), 2.85 (dd, J_{AB} 14.0, J_{BX} 7.1 Hz, 1H, CH$_A$$H_B$SH), 2.36–2.26 (m, 2H, CH$_2$C(O)), 2.22–2.15 (m, 2H, CF$_2$CH$_2$), 2.15–1.92 (m, 4H, C(O)NHCH$_2$CH_2 and CH_2CH$_2$NH$_3^+$), 1.92–1.82 (m, 4H, $^+$NH$_2$CH$_2$(CH_2)$_2$CH$_2$), 1.69–1.59 (m, 4H, CF$_2$CH$_2$CH_2 and CH$_2$C(O)), 1.49–1.28 (m, 12H, (CH_2)$_6$CH$_2$CH$_2$C(O)). ^{13}C NMR (DMSO, 125.8 MHz): δ 173.37 and 173.29 (*C*(O)NHCH), 171.28 and 171.19 (*C*(O)NHCH$_2$), 55.18 and 55.10 (C(O)NH*C*H), 46.01 and 45.96 ($^+$NH$_2$*C*H$_2$(CH$_2$)$_2$-*C*H$_2$NH$_2^+$), 44.41 (*C*H$_2$CH$_2$CH$_2$NH$_3^+$), 43.78 (C(O)NHCH$_2$CH$_2$*C*H$_2$), 36.04 (CH$_2$NH$_3^+$), 35.71 (C(O)NH-*C*H$_2$), 35.07 and 35.02 (*C*H$_2$C(O)), 29.57 (t, J 21.6 Hz, CF$_2$*C*H$_2$), 28.82, 28.73, 28.71, 28.61, 28.56, and 28.17 ((*C*H$_2$)$_6$CH$_2$CH$_2$C(O)), 25.88 (C(O)NHCH$_2$*C*H$_2$), 25.74 (CH$_2$SH), 25.10 (*C*H$_2$CH$_2$C(O)), 23.68 (*C*H$_2$CH$_2$NH$_3^+$), 22.59 and 22.55 ($^+$NH$_2$CH$_2$(*C*H$_2$)$_2$CH$_2$NH$_2^+$), 19.66 (t, J 3.5 Hz, CF$_2$CH$_2$*C*H$_2$). ^{19}F NMR (DMSO, 188.3 MHz): δ −77.23 (9F, CF$_3$COO$^-$), −83.12 (3F, CF$_3$), −116.12 (2F, CF$_2$CH$_2$), −125.98 (2F, CF$_3$CF$_2$CF_2), −127.74 (2F, CF$_3$CF_2). ESI-MS (positive mode): $(M + H)^+$ = 692.30 in agreement with the mass calculated for M = $C_{28}H_{50}F_9N_5O_2S$ (691.35).

CMC determination

The CMCs of the detergents were determined by a fluorescence enhancement method using the neutral fluorescent molecule 1,6-diphenyl-1,3,5-hexatriene (DPH).[42] Fluorimetric assays performed onto a Perkin Elmer spectrofluorimeter (LS 50 B) consisted in the measurements of the fluorescence intensity of a thermoregulated solution (25.0 ± 0.1 °C) of increasing detergent concentration in 1.5 mL of a nitrogen-saturated Hepes (20 mM, pH 7.4) buffer containing 5 μM DPH and 10 mM dithiothreitol (DTT). The solution was incubated for 20 min in the dark before measurement. The excitation and emission wavelengths were 358 and 430 nm, respectively. A plot of the fluorescence intensity *vs.* detergent concentration displayed a sharp break, and the corresponding concentration was taken as the CMC. The CMC of cetyltrimethylammonium bromide as control was also measured using this fluorimetric method and conditions (measured: 910 ± 50 μM; literature: 880 μM[42]).

Preparation of the [F-detergent]$_2$/DNA nanoparticles

A 5739 base-pair pCMV-control vector (pTG11236) encoding for the luciferase under transcriptional control of the SV40 promoter and enhancer regions was used in this study. pTG11236 was amplified by conventional methods. Basically, competent *E. coli* were grown at 37 °C for ~12–16 h (logarithmic growth phase) with vigorous shaking in LB media containing kanamycin. Bacteria were then harvested by centrifugation at 6000 *g* for 15 min at 4 °C. Cell residues were then subjected to appropriate plasmid purification protocol using Qiagen Giga kit endoxin free (following manufacturer specification notes). The quantities of detergent used were calculated according to the desired DNA concentration of 20 μg mL^{-1} (330 Da mean MW; 60 μM phosphate), the N/P ratio of the [F-detergent]$_2$/DNA complexes (N represents the number of amine equivalents of detergent, P the number of phosphate equivalents of DNA), the molar weight and the number of positive charges in the selected polycationic dimerizable detergent, as described elsewhere.[23,26]

As far as the preparation of the [F-detergent]$_2$/DNA complexes from the thiol detergents is concerned, all the solutions (DNA solution, Hepes, EtOH) were degassed using ultrasonic/N_2 cycles before use. DNA was diluted in Hepes (20 mM, pH 7.4) to a final concentration of 60 μM phosphate, then the desired amount of detergent was added from a freshly made EtOH stock solution (the concentration of the detergent in the stock solution was calculated so that the EtOH content in the final solution never exceeded 1% v/v). The [F-detergent]$_2$/DNA complexes were then formed by stirring the dispersions of the thiol detergent/DNA complexes in air at room temperature for 12 h to ensure fully cross-linking (thiol into disulfide oxidation), through air oxidation prior to further characterization experiments. For flow cytometry experiments, the plasmid DNA was labeled with YOYO (Molecular Probes, Eugene, USA) at a 1 YOYO per 150 base pairs (*i.e.* 38 molecules/plasmid) prior to its condensation with the detergents and labeling (next section).

Surface labeling or coating of the [F-detergent]$_2$/DNA nanoparticles

Decorated [F-detergent]$_2$/DNA complexes were obtained by adding the desired amount of [N-F6C10CysPEGFA]$_2$ conjugate (Fig. 2) from a DMSO stock solution to the above [F-detergent]$_2$/DNA complex dispersions (the concentration of the conjugate in the stock solution was calculated so that the DMSO content in the final solution never exceeded 1% v/v). The resulting solutions were kept at room temperature for at least 2 h before any characterization. The insertion equilibrium was reached within minutes as reported elsewhere in the case of liposomes.[43]

Measurement of the particle size by dynamic light scattering spectroscopy (DLS) and of the zeta potential by mixed mode measurement phase analysis light scattering (M3-PALS)

The measurements of the average particle size by DLS and zeta potential of the above samples (Hepes 20 mM, pH 7.4, DNA 60 μM phosphate or 20 μg mL^{-1}) were performed with a Zetasizer Nano ZS (Malvern) at 25 °C with the following specifications: sample time, 30 s; 10 measurements per sample; medium viscosity, 1.054 cP; refractive index of 1.33 and multimodal mode for DLS; medium dielectric constant of 80 and F(Ka) = 1.5 (Smoluchowsky) beam mode for zeta potential. Each formulation was reproduced in triplicate from newly prepared batches (DNA, F-detergent, conjugate) and each analysis was made in triplicate. Data given for one

formulation represent the mean (±SD) of all these measurements. The M3-PALS technique provided by the above apparatus allows also the zeta potential of the measurement cell (called wall zeta potential) to be determined. This potential is correlated to the colloidal stability of ionic formulations and their affinity for the solid interfaces, which are constituted by the wall of cell measurements. Indeed, M3-PALS experiments allow a clear distinction between the charge contribution due to the particles (*i.e.* the zeta potential of the particles) and the one due to the measurement cell (*i.e.* the wall zeta potential) by applying alternatively a fast field reversal measurement (to unambiguously determine the former) and a slow field reversal measurement (that allows for electro-osmosis assessment and then transposition into wall zeta potential).

Agarose gel electrophoresis

Each $[F\text{-detergent}]_2$/DNA sample (20 µl, 0.4 µg of plasmid) was electrophoresed for about 30 min under 150 V through a 0.8% agarose gel in TAE 1× (Tris-acetate-EDTA) buffer and stained by spreading a 2.5 µM ethidium bromide (Sigma) solution in TAE buffer. The DNA was then visualized on an UV transilluminator and photographed. The plasmid integrity in each sample was confirmed by electrophoresis after decomplexation with sodium dodecyl sulfate, as described elsewhere.[44]

Transmission electron microscopy (TEM)

Formvar-carbon coated grids previously made hydrophilic by glow discharge were placed on top of small drops of the (un)coated $[F\text{-detergent}]_2$/DNA samples (Hepes 20 mM, pH 7.4, DNA 60 µM phosphate or 20 µg mL^{-1}) prepared as described above. After 1–3 min of contact, grids were negatively stained with a few drops of 1% aqueous solution of uranyl acetate. The grids were then dried and observed with a Philips CM12 electron microscope working under standard conditions. All these experiments were reproduced twice on each formulation.

Cell culture

The RPMI 1640 (Gibco BRL) cell culture medium, if not indicated, was supplemented with 10% heated inactivated fetal bovine serum (FBS, Invitrogen), 2 mM glutamine (Sigma), 100 units mL^{-1} penicillin (Sigma) and 100 µg mL^{-1} streptomycin (Sigma). KB cells (human nasopharyngeal cancer cell line) were cultured in this medium at 37 °C in a 5% CO_2 humidified atmosphere. Overexpression of the folic acid receptor on KB cells (*i.e.* KB(+)) was induced by growing the cells (*i.e.* KB(−)) for three passages in folic acid depleted RPMI 1640 (Gibco BRL) as described elsewhere.[45]

In vitro transfection (luciferase assay)

24 h before transfection, KB(+) or KB(−) cells were seeded at a density of 2×10^4 cells/well in 96-well plates in RPMI 1640 without or with folic acid (2.27 µM), respectively, at 37 °C in a 5% CO_2 humidified atmosphere. 25 µL of the above described $[F\text{-detergent}]_2$/DNA (= pTG11236) and $[N\text{-F6C10CysPEG-FA}]_2$-coated $[F\text{-detergent}]_2$/DNA complexes or PEI/DNA N/P 5 polyplexes (positive control) were diluted to 100 µL in serum-free RPMI 1640 without or with folic acid (2.27 µM) in order to have 0.5 µg of DNA in the preparation (DNA concentration of 15 µM phosphate). The cell culture medium was removed and replaced by 100 µL of these DNA preparations (without folic acid for the KB(+) cells or with folic acid (2.27 µM) for the KB(−) cells). For the inhibition experiments, incubation was performed with DNA preparations containing 1 mM of folic acid. After 4 and 24 h, 50 and 100 µL of RPMI supplemented with 30% and 10% FBS, respectively, were added. After 48 h of incubation, the transfection was stopped, the culture medium was discarded, and the cells washed twice with 100 µL of PBS and lysed with 50 µL of lysis buffer (Promega, Charbonnières, France). The lysates were frozen −32 °C, awaiting analysis of luciferase activity. This measurement was performed on a TECAN luminometer in dynamic mode, for 10 s on 20 µL on the lysis mixture and using the "luciferase" determination system (Promega) in 96-well plates. Luciferase activity was calculated as femtograms (fg) of luciferase per milligram of protein. The total protein amount per well was determined by the BCA test (Pierce, Montluçon, France). The percentage of cell viability of the complexes was calculated as the ratio of the total protein amount per well of the transfected cells relative to that measured for untreated cells × 100%. The data were calculated from three or four repetitions in two fully independent experiments (formulation and transfection).

Cell uptake (flow cytometry)

The fluorescent YOYO-labeled, uncoated and coated $[F\text{-detergent}]_2$/DNA complexes were prepared as described above. 125 µL of these dispersions were diluted to 500 µL in serum-free RPMI (without folic acid for the KB(+) cells or with folic acid (2.27 µM) for the KB(−) cells) in order to have 0.5 µg of DNA in the preparation (DNA concentration of 15 µM phosphate). 24 h before cell uptake experiments, KB(+) and KB(−) cells were seeded at a density of 1×10^5 cells/well in 24-well plates RPMI 1640 without or with folic acid, respectively, at 37 °C in a 5% CO_2 humidified atmosphere. The culture medium was removed and replaced by 500 µL of the respective YOYO-labeled DNA complexes. For the inhibition experiments, incubation was performed with the YOYO-DNA preparations containing 1 mM of folic acid. After 4 h of incubation, the culture medium was discarded, and the cells washed twice with 500 µL of cold PBS, then incubated for 15 min at 37 °C in a 5% CO_2 humidified atmosphere with 1 mL of free serum RPMI containing 200 mg L^{-1} of calf thymus DNA to remove unspecific binding. Cells were then harvested by trypsination, resuspended in 500 µL of RPMI with 10% of FBS, collected by centrifugation (5 min, 2000 rpm), washed twice with 500 µL of cold PBS, and then resuspended in PBS/1% EDTA. Flow cytometry analysis was performed with a Ventage (Becton Dickinson, San Jose, CA, USA) using an argon laser (excitation at 488 nm for YOYO). Sorting windows were used on forward and side scatter to eliminate debris. Granulation, size and fluorescence intensity (emission 515 nm for YOYO) were recorded at a rate of 300 cells s^{-1}. Data were analyzed using winMDI 2.8 version software.

Statistical analysis

Analysis of the transfection/cell viability data as least square means with 95.0% confidence intervals was performed with STATGRAPHICS Plus5.0 software on the logarithmic transformation of transfection levels ($\log_{10}$(fg luciferase mg^{-1} protein)) and on the cell viability percentage. Analysis of variance (ANOVA) was also run on these data. Three factors, *i.e.* nature of the complexing agent (different F-detergent formulations, and PEI as control), N/P ratio, and presence or absence of folic acid, were analyzed as source of the variation of logarithmic transformation of the transfection levels using a multiple comparison procedure. The Least Significant Digit interval (LSD) method was used to discriminate among the means of the logarithmic transformation of luciferase expression levels.

Results and discussion

Synthesis and chemical stability of dimerizable cationic F-detergents

The synthesis of the dimerizable monocationic N-F4C10-CysTEGNH3 and tricationic N-F4C10CysSperlin detergents was performed successfully according to the straightforward procedure outlined in Scheme 1. It proceeded in three steps starting from the dimethylthiazolidine carboxylic acid **1**.[40] This synthon was first condensed with the perfluoroalkylated acid chloride generated *in situ* to give compound **2** (70% yield). The latter derivative was then reacted with BocNHTEG-OH 5 or *N*,*N*′,*N*″-triBoc-spermine **6**[41] in the presence of a strong activation coupling mixture (HOBt–EDC–DMAP) to give compounds **3** or **4** with 65 and 74% yield, respectively. Finally, deprotection of the *N*-Boc protecting groups as well as hydrolysis of dimethylthiazolidine ring was achieved almost quantitatively with an excess of TFA in dichloromethane affording N-F4C10CysTEGNH3 and N-F4C10CysSperlin, which were isolated as TFA salts.

This novel approach gave the desired compounds with overall yields in the 45–50% range. It contrasts strongly with the more tedious strategy that our group has reported for the synthesis of derivative N-F4C10CysSperlin[23] and briefly presented in Scheme 1 Path B. This approach used cystine methyl ester as starting material and proceeded in five steps to give the target derivative with an overall yield of ~7% only. The limiting step of this strategy was the coupling of two *N*,*N*′,*N*″-triBoc-spermine units **6** onto the cystine derivative **7**, which was performed in 20% yield.

To avoid oxidation of these thiol detergents into their disulfide lipids, they must be stored under a N_2 atmosphere. Moreover, for the preparation of stock solutions, one should preferably use ethanol wherein no oxidation occurred, and avoid DMSO wherein they were oxidized into their disulfide.[46] Indeed, ^{1}H NMR monitoring of the signals corresponding to CH cysteinyl (~4.3 ppm) or cystinyl (~4.5 ppm) related compounds over time in deuterated DMSO and at room temperature indicated that dimerization into the disulfide was almost complete within 4 h (data not shown). By contrast, in deuterated EtOH, the signal corresponding to the CH cysteinyl remained unchanged and no signal corresponding to the CH cystinyl was detected during this lapse of time.

It should further be emphasized that the oxidation of the thiol detergent into its disulfide lipid cannot be monitored by ESI-API MS. Indeed, the ESI-API MS analyses of the thiol detergents in DMSO solution poured into water–MeCN or water–MeOH mixtures were unsuccessful in detecting the disulfide over the thiol in the sample solution. Actually, ionization of the thiol monomers was several orders of magnitude over that of the oxidized disulfides. Consequently, if traces of thiol are still present in the disulfide sample, only the thiol and not the disulfide is detected by ESI-API MS. Moreover, in the case of the disulfide resulting from oxidation of N-F4C10CysTEGNH3, one would have expected m/z signals at 1275.52 for $(M + H)^+$ or 638.26 for $[(M + 2H)/2]^+$, which were not detected by ESI-API MS even when pure disulfide was injected.

CMC determination

The CMC of the N-F4C10CysTEGNH3 detergent, *i.e.* 190 μM, was determined in Hepes (20 mM, pH 7.4, 25.0 ± 0.1 °C) using a fluorimetric method based on DPH (5 μM) in the presence of DTT (10 mM) in order to avoid detergent oxidation, as described elsewhere for the N-F4C10CysSperlin and F4C11CysSperbr detergents.[23] This CMC value is surprisingly high as compared to that of N-F4C10CysSperlin (CMC = 85 μM) or F4C11CysSperbr (CMC = 130 μM) analogs. As these three derivatives possess a comparable perfluoroalkylated hydrophobic chain, the differences observed for their CMC values indicate that the TEGNH3 polar head is more hydrophilic than the tricationic linear spermine or tetracationic branched spermine polar head, respectively. The CMC value of N-F4C10CysTEGNH3 is also unexpectedly high as compared to that of the hydrocarbon dicationic C14CysOrn analog (CMC = 45 μM; see structure in Fig. 1). This shows that the increase of hydrophobicity resulting from the replacement of a hydrocarbon $H(CH_2)_{14}$ chain for a more hydrophobic $F(CF_2)_4(CH_2)_{11}$ one (whose contribution to micellization is equivalent to a $H(CH_2)_{17}$ chain)[24] is largely compensated by the increase of hydrophilicity resulting from the replacement of the dicationic ornithine by the TEGNH3 polar head.

We also tried to measure the CMC values for the dimer resulting from the oxidation of the thiol N-F4C10Cys-TEGNH3 into its disulfide lipid. Unfortunately, the DPH-based fluorescence method failed, its CMC or aggregation concentration being far below the limit of this technique (1 μM). This result is in line with those reported for the dimers of the hydrocarbon[18] and perfluoroalkylated detergents[23] shown in Fig. 2. It indicates however that the [N-F4C10-CysTEGNH3]$_2$ lipid dimer displays a much lower CMC than its corresponding monomer detergent and, consequently, that DNA can be condensed into monomolecular nanoparticles by the monomer cationic detergent, which can then be stabilized by subsequent dimerization of the detergent into its lipid on the DNA matrix.

With respect to attain monomolecular cationic DNA nanoparticles at a concentration of 60 μM (expressed as phosphate equivalents, P) for transfection experiments, the three

perfluoroalkylated detergents were candidates for DNA condensation in aggregation-free conditions. To provide monomolecular DNA condensation, the excess of free cationic detergent was kept close to its CMC. For a DNA concentration of 60 μM, this is the case when the N/P ratio of total detergent (expressed as amine equivalents, *N*) to DNA (expressed as *P* equivalents) is ≤ 3 for the monocationic N-F4C10CysTEGNH3, ≤ 4 for the tricationic N-F4C10-CysSperlin, and ≤ 8 for the tetracationic F4C11CysSperbr.

Plasmid DNA condensation—particle formation and characterization

Various DNA (pTG11236) complexes were formulated from EtOH solutions of the three perfluoroalkylated N-F4C10-CysTEGNH3, N-F4C10CysSperLin, F4C11CysSperBr detergents, for a plasmid concentration of 60 μM phosphate, and for N/P ratios ranging from 0.8 to 5. The resulting particles were then stabilized by oxidation (air (O_2) atmosphere and at room temperature for 12 h) of every two detergents into a $[\text{detergent}]_2$ lipid molecule, within the DNA-associated micelles. Under such aerobic conditions and in the presence of DNA template, oxidation of the thiol detergent into lipid disulfide occurred within 6 h.[18] Dynamic light scattering (DLS) for average size measurements and zeta potential measurements by M3-PALS analyses were then performed on the resulting stabilized $[\text{F-detergent}]_2$/DNA formulations. These data (means and standard deviation), which result from three different and distinct experiments (different batches of plasmid and detergent), each formulation and measurement being further realized in triplicate, were plotted for better convenience as shown in Fig. 3. The resulting stabilized $[\text{F-detergent}]_2$/DNA complexes were also analyzed by agarose gel electrophoresis (see below, Fig. 5) and by TEM.

Results obtained for the zeta potential measurements showed a conventional behavior of the $[\text{F-detergent}]_2$/DNA formulations, *i.e.* zeta potential increasing with regard to N/P. Indeed, all the three plots followed a nice sigmoid curve pattern (Fig. 3). With the monocationic N-F4C10-CysTEGNH3 and tricationic N-F4C10CysSperlin detergents, negative (≤ -40 mV) and positive zeta potential values ($\leq +40$ mV) were measured for the $[\text{F-detergent}]_2$/DNA complexes for $N/P \leq 1.5$ and ≥ 3, respectively. These N/P values were shifted to 2 and 3.5, respectively, for the tetracationic F4C11CysSperbr-based DNA ones. For these negative/positive zeta potentials and corresponding N/P values, the $[\text{F-detergent}]_2$/DNA complexes displayed sizes in a narrow 40–80 nm range (excepting for the F4C11CysSperbr N/P 5 formulation: 100 nm) and consisted into a monodisperse population of nanoparticles. These results were further confirmed by TEM experiments (data not shown; see also next section).

Neutrality of the $[\text{F-detergent}]_2$/DNA complexes was obtained at $N/P \sim 2$ with the monocationic N-F4C10Cys-TEGNH3 and tricationic N-F4C10CysSperlin, and at $N/P \sim 3$ with the tetracationic F4C11CysSperbr. Concomitantly, and as generally observed for particles of zeta potential close to neutrality, colloidal instability with aggregation and precipitation was noticed.

That DNA condensation leading to particles/aggregates exhibiting a zeta potential close to 0 mV occurred at N/P ratios higher than 1 and at different N/P ratios with respect to the nature of detergents/lipids, suggests that active auto-assembling driving forces between the detergent/lipid molecules and hydrophobic interactions are of prime importance for the DNA compaction process. With increasing the N/P ratio from 0.8 to 5, DNA is first compacted into negatively charged particles (wherein DNA is exposed on the particle's surface; see next section), then into neutral ones, and finally into cationic nanoparticles wherein DNA is entirely covered/protected by the detergent/lipid layer. This can only be achieved when a minimum number of cationic detergent (lipid) molecules are present and self-organize on the DNA matrix into systems (micelles, mono-(bi)layers). This is why, for a given DNA amount (*i.e.* expressed by *P*), a N/P ratio higher than 1 is required for neutrality. This is also why a higher N/P ratio, hence a higher concentration, for the F4C11CysSperbr (*i.e.* expressed by *N*) than for N-F4C10CysTEGNH3 or N-F4C10CysSperlin is required to compact DNA. Indeed, at a given N/P ratio and DNA concentration, the concentration of the monocationic N-F4C10CysTEGNH3 is three-fold that of the tricationic N-F4C10CysSperlin, and four-fold that of the tetracationic F4C11CysSperbr.

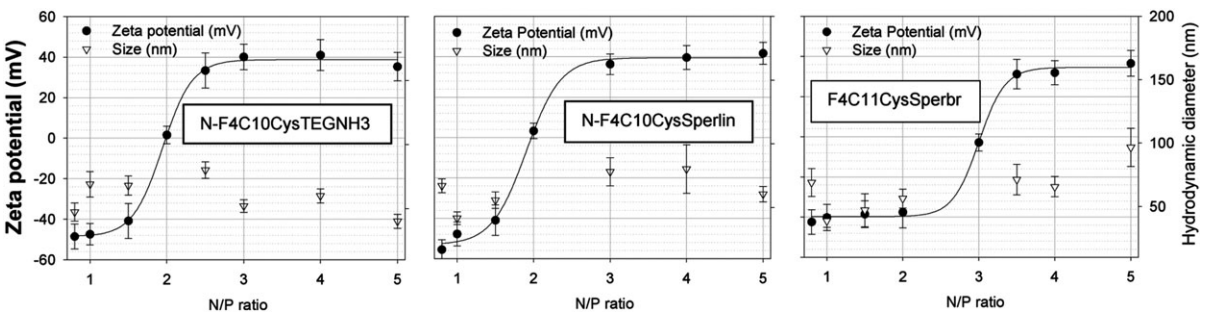

Fig. 3 Zeta potential (in mV) and hydrodynamic diameter (in nm) of the $[\text{F-detergent}]_2$/DNA complexes formulated with the N-F4C10Cys-TEGNH3, N-F4C10CysSperlin, or F4C11CysSperbr detergent as a function of the N/P ratio (*N*, number of amine equivalents of the detergent; *P*, number of DNA phosphate equivalents). Complexes were prepared in Hepes 20 mM, pH 7.4. Measurements were performed on samples containing 60 μM phosphate of DNA (20 μg mL^{-1}). The polydispersity index of the formulations shown ranged from 0.18 to 0.38 for N-F4C10CysTEGNH3, from 0.26 to 0.45 for N-F4C10CysSperlin, and from 0.14 to 0.36 for F4C11CysSperbr. For more details, see Experimental section.

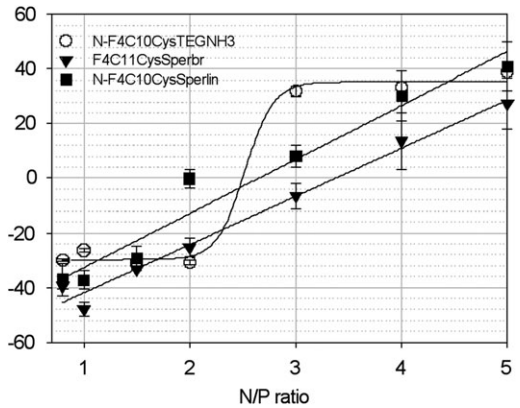

Fig. 4 Zeta potential of the measurement cell wall containing the [F-detergent]$_2$/DNA complexes formulated with the N-F4C10CysSperlin, N-F4C10CysTEGNH3, or F4C11CysSperbr detergent, as a function of their N/P ratio. For more details, see caption of Fig. 3.

This analysis seems further to be corroborated by the wall zeta potential evolution of the measurement cell with regard to N/P, hence with regard to the concentration of lipid, the DNA concentration in the samples being constant. As shown in Fig. 4, the wall zeta potential of the measurement cell for the [F-detergent]$_2$/DNA formulations made from the tri- or tetracationic F-detergents increased gradually and almost linearly with respect to N/P and reached a maximum at $\sim +40$ mV for $N/P \geq 4$ and 5 for N-F4C10CysSperlin and F4C11CysSperbr, respectively. This pattern indicates that these two condensing agents (as their lipid disulfide) exchange extensively between the [F-detergent]$_2$/DNA complexes and bulk solution, and contribute to modify the surface charge of both the [F-detergent]$_2$/DNA complexes and the measurement cell wall. By contrast, with N-F4C10CysTEGNH3, one observed a sigmoid pattern, the wall zeta potential of the measurement cell remaining unaffected for a N/P value of up to 2, then a rapid increase to attain a plateau at N/P 3. This behavior indicates that for N/P ratio ≤ 2, N-F4C10CysTEGNH3 contributed likely to the DNA compaction process only. That saturation of the cell wall occurs at a lower N/P ratio for N-F4C10CysTEGNH3 than for N-F4C10CysSperlin and F4C11CysSperbr (indicating a higher concentration of its lipids in bulk solution), is indeed expected as, at a given N/P ratio, the concentration of the monocationic N-F4C10CysTEGNH3 is three- and four-fold higher than that of tricationic N-F4C10CysSperlin and tetracationic F4C11CysSperbr, respectively.

Concerning the monocationic N-F4C10CysTEGNH3 condensing agent, one can further envisage an active role of the triethyleneoxy moiety, which could contribute to modify hydration structure. It is well known that hydration forces greatly affect biomolecular systems.[47] The reconfiguration of the water shell at the DNA–bulk interface by the triethyleneoxy moiety, in combination with the electrostatic condensation process induced by the terminal ammonium, could result into an efficient DNA collapse.

The major advantage of utilizing cationic detergents over lipids or polymers for compacting DNA relies on the "monomolecular" condensation process, which guides the DNA compaction, because of reversible DNA/detergent interactions, fast exchange between detergent in complexes and in bulk/micelles, and entropy consideration, towards the highest number of particles, hence one DNA copy per complex.[21,22] Theoretically, one should obtain particles displaying a mean diameter size in the 30–50 nm range with respect to the size of the used DNA ($\sim$5739 bp) and in case of a monomolecular condensation process.[48] Our DLS data, which showed the presence of a monodisperse population of very small-sized particles (ranging from 40 to 80 nm) for a N/P ratio outside the range for which zeta potentials were close to neutrality, revealed that likely monomolecular DNA particles but also particles containing a few copies of DNA have formed.

It should be emphasized that surprisingly, part of these results concerning the polycationic detergent-based formulations differs to some extent from those our group has previously reported.[23] The experimental conditions and mostly the fact that the DNA compaction was performed from detergent stock solution in ethanol (this study) and not in DMSO[23] account for these differences. Indeed, as demonstrated by ^{1}H NMR (see synthesis section), we found out that in DMSO the thiol detergents were partly oxidized into its disulfide. Moreover, when we repeated the formulation process as described in our previous report (hence from detergent stock solution in DMSO), we reproduced our former results.

The resulting stabilized [F-detergent]$_2$/DNA complexes made with the perfluoroalkylated detergents were also

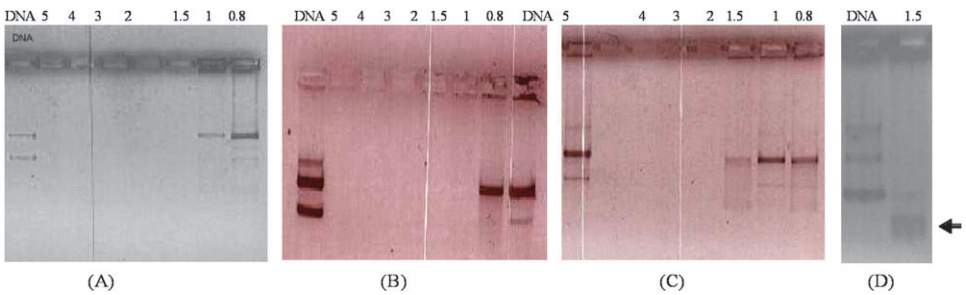

Fig. 5 Agarose gel electrophoresis of the [F-detergent]$_2$/DNA complexes formulated with the N-F4C10CysSperlin (A and D), N-F4C10-CysTEGNH3 (B), or F4C11CysSperbr (C) detergent at various N/P ratios. For experiments A–C, 20 μL (0.4 μg of DNA) of sample containing DNA at a concentration of 20 μg mL^{-1} (60 μM) was deposited. For experiment D, [N-F4C10CysSperlin]$_2$/DNA N/P 1.5 complexes were prepared at a DNA concentration of 180 μM, and 20 μL (1.2 μg of DNA) of this sample was deposited. The presence of a band migrating faster than DNA (arrow) indicates the presence of compacted, stable and negatively charged particles. Staining was performed by spreading of ethidium bromide.

analyzed by agarose gel electrophoresis (Fig. 5) for assessing DNA complex formation as well as DNA integrity. Lipoplexes (DNA complexes made up from cationic lipids) or polyplexes (DNA complexes made up from cationic polymers) are known to remain in the loading well, even for N/P ratios below or close to 1. The $[C14CysOrn]_2$/DNA nanoparticles formed at N/P ratios of 0.6–1.2 and after oxidation of the condensing cationic C14CysOrn detergent (see structure in Fig. 1) were however found to be mobile and to move faster than free DNA.[18,19] These experiments were taken to indicate that monomolecular DNA condensation into highly compacted stable particles that bear further a negative surface charge had occurred.

Though faint, bands moving faster than free, uncomplexed DNA could nevertheless been detected for the N/P 0.8, 1 and 1.5 $[F\text{-detergent}]_2$/DNA complexes formulated with the three perfluoroalkylated detergents reported here after subsequent stabilization through oxidation (Fig. 5(A)–(C)). The presence of highly compacted, stable and negatively charged particles was further confirmed by the presence of a band migrating faster than DNA, as clearly evidenced by gel electrophoresis performed on a more concentrated N/P 1.5 formulation made from N-F4C10CysSperlin and 180 μM DNA (Fig. 5(D)). Furthermore, the detection of these bands indicates that DNA is accessible for ethidium bromide intercalation and exposed onto the surface of these negatively charged monomolecular nanoparticles.

However, the gel electrophoresis experiments indicated rather a conventional behavior similar to that of cationic lipoplexes and polyplexes, hence (i) particles remaining in the loading well with the presence of free and/or complexed DNA but accessible for ethidium bromide intercalation for a N/P ratio ≤ 1 (1.5 for F4C11CysSperbr), and (ii) particles remaining in the loading well with the presence of fully complexed DNA (not accessible for ethidium bromide intercalation) for a N/P ratio ≥ 2. That a higher N/P ratio to complex all DNA was required for the tetraamine F4C11-CysSperbr than for the two other compounds supports the idea that a minimum number of cationic detergent (lipid) molecules is required to self-organize on the DNA matrix for its full condensation into a compacted state.

The plasmid integrity in each formulation made from the three perfluoroalkylated detergents and after oxidation was further confirmed by agarose gel electrophoresis after decomplexing the $[F\text{-detergent}]_2$/plasmid particles with sodium dodecyl sulfate (SDS), *i.e.* electrophoretic mobility of SDS-released DNA is identical to that of naked DNA (data not shown).

Characterization of labeled $[F\text{-detergent}]_2$/DNA nanoparticles

The second objective of this work was to coat the $[F\text{-detergent}]_2$/DNA nanoparticles with the amphiphilic-PEG-folic acid conjugate, $[N\text{-F6C10CysPEG-FA}]_2$,[28] shown in Fig. 2. This step and its unambiguous characterization is most important for further experiments aimed at evidencing cell receptor mediated endocytosis of the folic acid-labeled monomolecular DNA nanoparticles. For these studies, we selected (i) the negatively charged $[F\text{-detergent}]_2$/DNA complexes formulated from N-F4C10CysTEGNH3 and N-F4C10CysSperlin at a N/P ratio of 1.5, and (ii) the positively charged ones made from these two detergents at a N/P ratio of 3 and 4, and from F4C11CysSperbr at a N/P ratio of 4 and 5. These formulations were more particularly chosen for their very low particle sizes (see precedent section). For their labeling, the nanoparticles, once they have been prepared, were incubated with various amounts (from 0.5 to 5 mol% with regard to the detergent) of the amphiphilic-PEG-Folic acid conjugate. Post-decoration of the particles was followed by zeta potential and size measurements. These data shown in Fig. 6 were recorded once the equilibrium was attained ($\sim$2 h of incubation at 25 °C).[43] The sizes and morphologies of the coated $[F\text{-detergent}]_2$/DNA complexes was also examined by TEM (Fig. 7).

Unreproducible and erratic results in terms of particle size and zeta potential were obtained for only the negatively charged N/P 1.5 $[N\text{-F4C10CysTEGNH3}]_2$/DNA nanoparticles to which 2 or 5% mol of conjugate was added. This is probably related to the fact that the conjugate at the concentration corresponding to 2% mol in the sample (*i.e.* 8×10^{-4} μM) is already forming supramolecular assemblies, which are destabilizing the DNA complexes. These assemblies consist likely into micelles. Indeed, DLS measurements performed onto buffer solutions containing only the conjugate at various concentrations showed that, for a conjugate concentration $\geq 8 \times 10^{-4}$ μM, these solutions consisted into a suspension of a monodisperse population of 15 nm-sized aggregates. Moreover, accessibility of the hydrophobic lipid domains within the negatively charged $[N\text{-F4C10Cys-TEGNH3}]_2$/DNA nanoparticles is probably restricted by the hydrophilic negatively-charged shield provided by DNA exposed onto their surface. One can therefore expect a slow exchange of the conjugate (which is negatively charged at pH 7.4) between the micelles in bulk and the hydrophobic lipid domains in complexes. This is not the case for the positively charged $[F\text{-detergent}]_2$/DNA nanoparticles whose external surface consists into a cationic lipid layer and for which a fast exchange of the conjugate from the micelles in bulk (if present) to the hydrophobic lipid domains on the surface of the complex can take place. This exchange is further favored by a close contact resulting from attractive electrostatic interactions between the negatively charged conjugate/micelles and the positively charged surface of the nanoparticles.

Evidences as for post-decoration of both the negatively and positively charged $[F\text{-detergent}]_2$/DNA nanoparticles by the amphiphilic-PEG-folic acid conjugate really occurred were dispelled since their initial zeta potential was increasing and decreasing, respectively, with increasing the amount of conjugate added, as expected from the shielding of the nanoparticle's charge surface by PEG. For the N/P 1.5 negatively charged $[F\text{-detergent}]_2$/DNA nanoparticles, zeta potential increased from ~ -40 mV (naked nanoparticles) to a plateau of ~ -15 mV for N-F4C10CysTEGNH3 (Fig. 6(a)) and ~ -20 mV for N-F4C10CysSperlin (Fig. 6(b)) on adding conjugate, indicating almost saturation of the nanoparticle's surface by the conjugate. For the positively charged $[F\text{-detergent}]_2$/DNA nanoparticles, zeta potential decreased from $\sim +40$ mV (naked nanoparticles) to a value of $\sim +5$ to $+15$ mV for 5 mol% of conjugate (Fig. 6(a)–(c)).

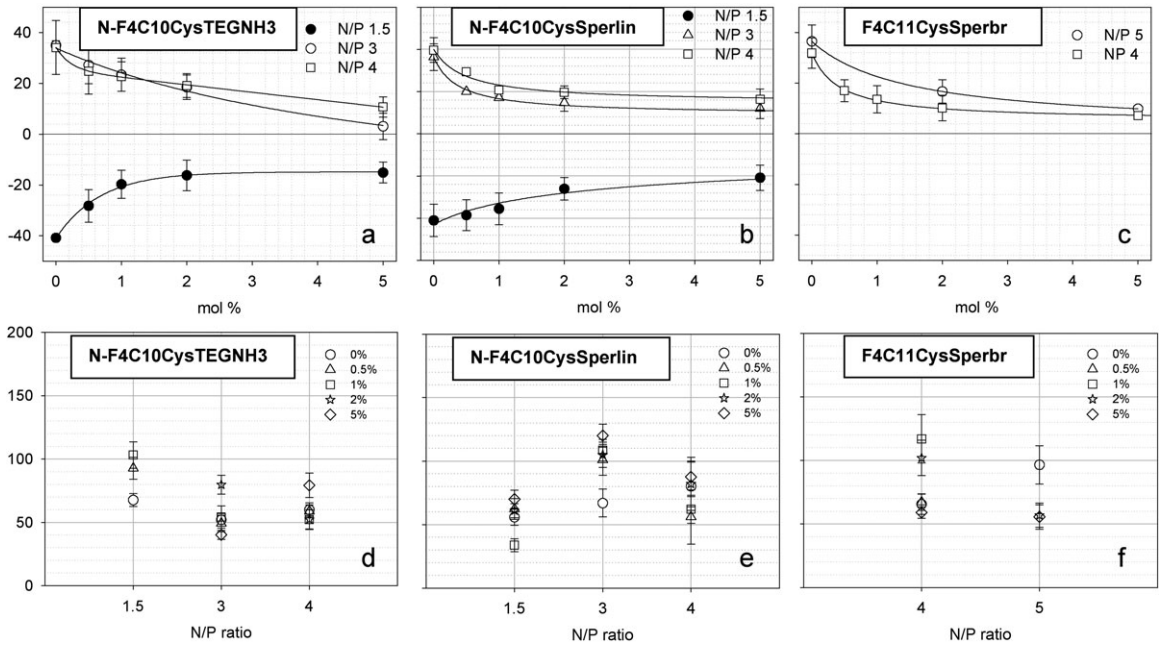

Fig. 6 Labeling of the [F-detergent]$_2$/DNA nanoparticles formulated with the N-F4C10CysTEGNH3, N-F4C10CysSperlin or F4C11CysSperbr detergent. Zeta potentials ((a)–(c)) and hydrodynamic diameters ((d)–(f)) of the [F-detergent]$_2$/DNA nanoparticles as a function of increasing amounts of [N-F6C10CysPEG-FA]$_2$ and for various N/P ratios. Complexes (DNA 60 μM, 20 μg mL^{-1}) were prepared in Hepes 20 mM, pH 7.4 at the indicated N/P ratio, and incubated with 0.5 to 5 mol% of [N-F6C10CysPEG-FA]$_2$ conjugate with regard to the detergent. The polydispersity index of the coated formulations shown ranged from 0.21 to 0.38 for N-F4C10CysTEGNH3, from 0.12 to 0.31 for N-F4C10CysSperlin, and from 0.14 to 0.28 for F4C11CysSperbr. For more details, see Experimental section.

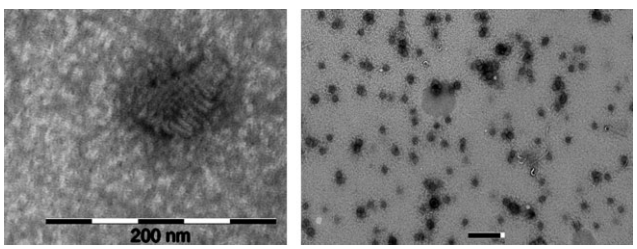

Fig. 7 Transmission electron microscopy of [N-F4C10CysTEGNH3]$_2$/DNA N/P 4 complexes coated with 2 mol% of [N-F6C10CysPEG-FA]$_2$ in Hepes 20 mM, pH 7.4 and at a DNA concentration of 60 μM phosphate (20 μg mL^{-1}). Left: morphology of a single DNA nanoparticle (bar = 200 nm); right: general view of the grid (bar = 400 nm).

Concerning the effect of conjugate on the negatively and positively charged [F-detergent]$_2$/DNA nanoparticle's size, it appeared, as illustrated in Fig. 6(d)–(f), that sizes remained in most cases unaffected by the presence of the conjugate (excepting for the N/P 1.5 [N-F4C10CysTEGNH3]$_2$/DNA nanoparticles incubated with 2 and 5 mol% of conjugate, as discussed above). When a particle size increase was observed (see Fig. 6(d), (e) and (f) for N/P 1.5, 3 and 4, respectively), the size increase remained however modest and the sizes remained below 140 nm. To confirm these results, TEM analyses were also performed. Unfortunately, formulations containing 5 mol% of conjugate did not adhere onto the grids, thus preventing TEM analyses. However, and as illustrated in Fig. 7 for the N/P 4 [N-F4C10CysTEGNH3]$_2$/DNA nanoparticles incubated with 2 mol% of conjugate, TEM experiments indicated the presence of a homogenous population of compact nanoparticles with sizes below 100 nm in full agreement with the DLS measurements reported in Fig. 6. Furthermore, the TEM pictures obtained for the coated nanoparticles (Fig. 7) were very similar to those obtained for the uncoated ones (not shown). Moreover, at higher magnification (Fig. 7, left), a tubular ultrastructure similar to that reported for monomolecular DNA nanoparticles[18] was seen.

Cell targeted transfection properties of coated [F-detergent]$_2$/DNA nanoparticles

Our main objective was to demonstrate that targeted quasi-monomolecular [F-detergent]$_2$/DNA nanoparticles coated with the amphiphilic-PEG-folic acid conjugate, bearing whether a negative or a positive surface charge, were able to specifically deliver genes to cells overexpressing folate receptors. However, cationic DNA complexes also provide receptor-independent gene transfer into cells (and more particularly into adherent cells). This process involves electrostatic interactions between the cationic DNA particles and the anionic cell proteoglycans expressed on the cell surface.[49,50] It was therefore necessary to determine the conditions under which a non-specific gene transfer process into cells, whether over-expressing folate receptors or not, can occur with the unlabeled and labeled [F-detergent]$_2$/DNA nanoparticles. To evaluate the "non-specific" transfection potential of the targeted formulations into folate(−) cells and to further minimize the non-specific transfection pathway into folate(+) cells, we selected KB cells which over-express folate receptors when cultured in folic acid depleted media.

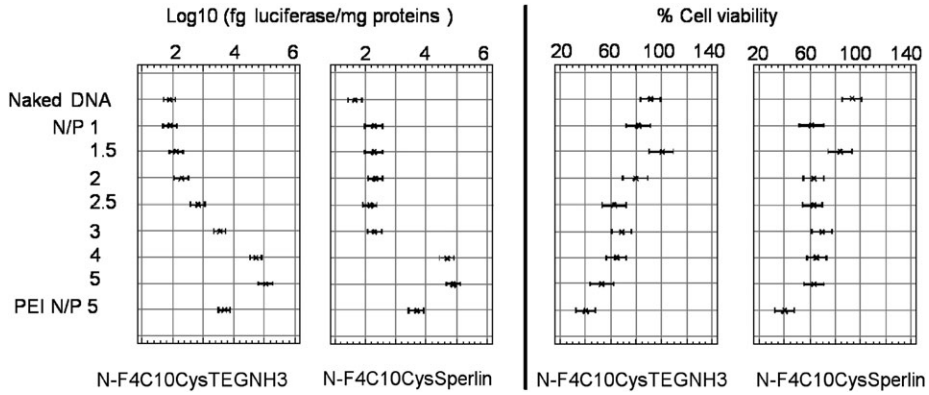

Fig. 8 Transfection (least square means with 95.0% confidence intervals of the logarithmic transformation levels $-\log_{10}$(fg luciferase mg^{-1} protein) and cell viability of KB(−) cells mediated with the $[F\text{-detergent}]_2$/DNA (= pTG11236) nanoparticles formulated with the N-F4C10CysTEGNH3 or N-F4C10CysSperlin detergent in comparison with branched PEI (25 kDa) based polyplexes and naked pDNA, and for a pDNA dose of 0.5 μg/well (15 μM phosphate). pDNA was mixed with the detergent at the indicated N/P ratio, then oxidized as described in the Experimental section, then placed in the wells onto the KB(−) cells. For more details, see Experimental section.

Among the above-described formulations, we selected the $[N\text{-F4C10CysSperlin}]_2$/DNA and $[N\text{-F4C10CysTEGNH3}]_2$/DNA complexes exhibiting (i) a negative (N/P 1 and 1.5), neutral (N/P 2) or positive ($N/P \geq 2.5$) zeta potential, and (ii) a mean particle size in the 40–80 nm range. A series of control experiments was first realized with naked DNA (= pTG11236, a pCMV-luciferase encoding plasmid), non-targeted DNA complexes, and PEI-based N/P 5 DNA polyplexes on KB(−) and KB(+) cells. A second series of control experiments was also performed with the $[N\text{-F6C10CysPEGFA}]_2$-coated DNA complexes on KB(−) cells. The transfection efficiency of these DNA complexes (expressed in femtograms (fg) of luciferase mg^{-1} of protein) was further evaluated (i) in the absence or presence of an excess of folic acid (1 mM), (ii) in the absence of serum, and (iii) for a DNA dose of 0.5 μg/well (15 μM phosphate). Transfection was investigated at such a low DNA concentration, because such diluted conditions are particularly more relevant for evidencing a transfection enhancement resulting from folate-mediated endocytosis when *in vivo* uses are contemplated. It should also be emphasized that, to highlight unambiguously a specific uptake into cells *via* the folate receptor, the nanoparticles were incubated with the cells in the absence of any extra components (*e.g.* serum), which were susceptible to interfere with the uptake process. The cell viability of the DNA complexes was also checked by determining the total protein amount per well of the transfected cells relative to that measured for untreated cells.

The results concerning the transfection and cell viability of the control experiments on KB(−) and KB(+) cells with the unlabeled $[F\text{-detergent}]_2$/DNA and their statistical analyses are illustrated in Fig. 8 and 9, respectively. Importantly, the statistical analysis of the transfection data indicated that the $[N\text{-F4C10CysSperlin}]_2$/DNA and $[N\text{-F4C10CysTEGNH3}]_2$/DNA complexes do allow DNA transfection of KB(−) cells only for $N/P \geq 4$ and 2.5, respectively, *i.e.* for nanoparticles bearing a positive zeta potential. Moreover, transfection is already optimal for a N/P ratio of 4, and with an efficiency at least, one order of magnitude higher than that of the N/P 5 PEI polyplexes (Fig. 8). It should further be noted that these $[F\text{-detergent}]_2$/DNA nanoparticles display a cell viability still close to 70% and higher than that of the PEI polyplexes (40%). All these observations together led us to foresee a non-specific endocytosis mechanism proceeding by electrostatic interactions between the cationic unlabeled $[F\text{-detergent}]_2$/DNA nanoparticles and the anionic proteoglycans expressed at the cell membrane of these adherent KB(±) cells. Taking into account that the $[F\text{-detergent}]_2$/DNA formulations consisted mainly into a population of quasi-monomolecular DNA nanoparticles of very low size, these results are particularly remarkable.

Importantly also, our results show that the over-expression of the folate receptor has either no effect or rather a deleterious impact on the non-specific transfection of KB cells when mediated with the $[N\text{-F4C10CysSperlin}]_2$/DNA or $[N\text{-F4C10CysTEGNH3}]_2$/DNA complexes, respectively. Indeed, comparable luciferase levels were noticed on both the KB(−) and KB(+) cells for the $[N\text{-F4C10CysSperlin}]_2$/DNA formulation, while much lower levels were measured with the $[N\text{-F4C10CysTEGNH3}]_2$/DNA complexes in the KB(+) cells than in the KB(−) cells (Fig. 9).

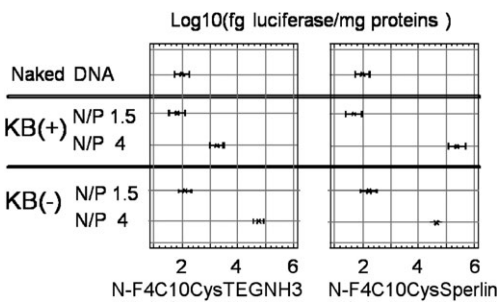

Fig. 9 Transfection (least square means with 95.0% confidence intervals of the logarithmic transformation levels $-\log_{10}$(fg luciferase mg^{-1} protein) of KB(+) cells mediated with the $[F\text{-detergent}]_2$/DNA (= pTG11236) nanoparticles formulated with the N-F4C10CysTEGNH3 or N-F4C10CysSperlin detergent for a N/P ratio of 1.5 or 4, and for a pDNA dose of 0.5 μg/well (15 μM phosphate), in comparison with the data collected on the KB(−) cells. For more details, see caption of Fig. 7 and Experimental section.

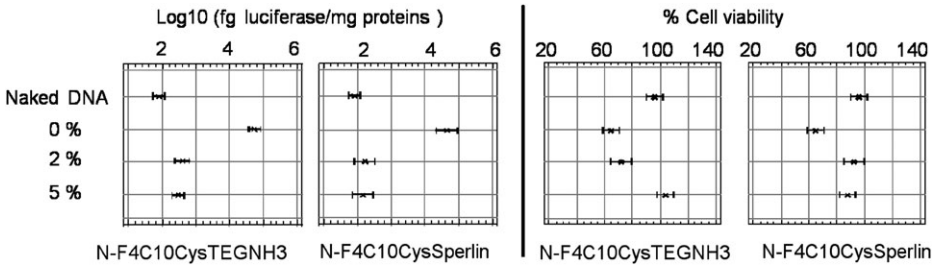

Fig. 10 Transfection (least square means with 95.0% confidence intervals of the logarithmic transformation levels $-\log_{10}$(fg luciferase mg^{-1} protein) and cell viability of KB(−) cells mediated with the [N-F6C10CysPEG-FA]$_2$-labeled [F-detergent]$_2$/DNA(= pTG11236) nanoparticles formulated with the N-F4C10CysTEGNH3 or N-F4C10CysSperlin detergent at a N/P ratio of 4, as a function of increasing amounts of [N-F6C10CysPEG-FA]$_2$, and for a pDNA dose of 0.5 μg/well (15 μM phosphate). The [F-detergent]$_2$/DNA nanoparticles were incubated with 2 or 5 mol% of [N-F6C10CysPEG-FA]$_2$ conjugate with regard to the detergent, then placed in the wells onto the KB(−) cells. For more details, see Experimental section.

Concerning the control experiments related to the transfection of KB(−) cells with the [N-F6C10CysPEGFA]$_2$–labeled [F-detergent]$_2$/DNA nanoparticles, our data illustrated in Fig. 10 for the N/P 4 formulations showed that the presence of increasing amounts of [N-F6C10CysPEGFA]$_2$ conjugate (from 2 to 5 mol% per mol of detergent) resulted in a dramatic decrease of the luciferase expression levels and in a concomitant cell viability increase, as expected. This is in line with several reports in literature indicating that the PEG coating of cationic DNA nanoparticles results in the hiding of their cationic surface, thus preventing the electrostatic interactions with the cell anionic proteoglycans to take place, and, consequently, cell uptake. It should further be emphasized that the resulting luciferase level decrease and cell viability increase with increasing amounts of conjugate confirm the [F-detergent]$_2$/DNA nanoparticle's coating by the conjugate.

Whether the coating of the [F-detergent]$_2$/DNA nanoparticles with the [N-F6C10CysPEGFA]$_2$ conjugate resulted into an increase of luciferase expression, as a result of a specific receptor(folate)-mediated endocytosis, our data illustrated in Fig. 11 for the cationic N/P 4 formulations showed that this is not the case. Indeed, although higher luciferase levels (one order of magnitude) were measured for the KB(+) cells than for the KB(−) ones when transfected with the targeted N/P 4 [N-F4C10CysSperlin]$_2$/DNA nanoparticles (Fig. 11), no transfection inhibition was however observed when the experiments were performed in the presence of excess folic acid (1 mM). As for the targeted N/P 4 [N-F4C10CysTEGNH3]$_2$/DNA nanoparticles (Fig. 10), though a decrease of luciferase expression in the KB(+) cells was noticed in the presence of folic acid, a comparable effect was, however, also observed with the KB(−) cells, indicating that cell uptake and transfection with these formulations were not specific.

It should further be emphasized that the coating of the negatively charged N/P 1.5 formulations (which provided an ideal matrix for limiting the non-specific electrostatic interactions with cells) did not increase their transfection ability, the luciferase levels measured being close to those obtained with naked plasmid (data not shown). This result, although disappointing, is however in line with another report in literature.[19]

Several reasons may account for these contrasting results: (i) non-specific cell uptake of the targeted [F-detergent]$_2$/DNA nanoparticles into the KB(+) cells, (ii) poor specific ligand-receptor interactions, resulting into no or poor receptor-mediated endocytosis, (iii) effective specific ligand-receptor interactions triggering receptor-mediated endocytosis into intracellular compartments but from which the nanoparticles cannot escape into the cytosol, and/or (iv) poor intracellular trafficking from the cytosol into the nucleus.

In order to have a closer insight into the different events occurring between the targeted [F-detergent]$_2$/DNA nanoparticles and the KB(±) cells, we investigated their interactions and cell uptake by fluorescence-activated cell sorting (FACS). These FACS analyses were performed with the [N-F4C10CysTEGNH3]$_2$/DNA nanoparticles, at a N/P ratio of 1.5 and 4, and for an amount of conjugate of 0.1 and 5 mol%. For these experiments, the plasmid was first tagged by the fluorescent DNA-intercalating dye YOYO-1 (38 molecules/plasmid). The YOYO-labeled (un)targeted [F-detergent]$_2$/DNA nanoparticles were then formed as described for the unlabeled ones. The KB(±) cells were then incubated with the YOYO-labeled (un)targeted [F-detergent]$_2$/DNA nanoparticles under the same conditions as those used for the first part of the luciferase assays, *i.e.* same number of cells per mL, 4 h of incubation, absence of serum, absence or presence of free folic acid (1 mM), and a DNA concentration

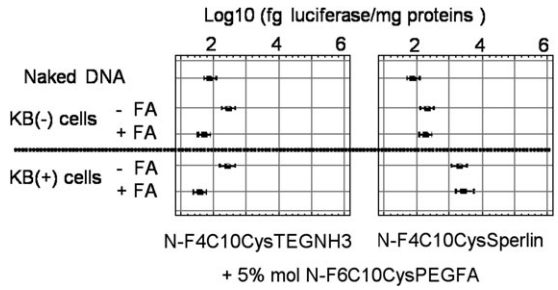

Fig. 11 Transfection (least square means with 95.0% confidence intervals of the logarithmic transformation levels $-\log_{10}$(fg luciferase mg^{-1} protein) of KB(+) and KB(–) cells mediated with the [N-F6C10CysPEG-FA]$_2$-labeled [F-detergent]$_2$/DNA(= pTG11236) nanoparticles formulated with the N-F4C10CysTEGNH3 or N-F4C10CysSperlin detergent for a N/P ratio of 4, a DNA dose of 0.5 μg/well (15 μM phosphate), and in the absence (−) or presence (+) of 1 mM folic acid (FA). For more details, see Experimental section.

of 15 μM phosphate. After 4 h of incubation with the DNA nanoparticles, the cells were washed and then incubated with a calf thymus DNA solution to remove unspecific binding, and only living cells were analyzed by FACS (for more details see the experimental procedure section).

For the negatively-charged N/P 1.5 [N-F4C10Cys-TEGNH3]$_2$/DNA nanoparticles whether targeted or not, no differences of fluorescence intensity associated to the KB(+) cells were noticed between the untreated and treated KB(+) cells (data not shown), indicating a very poor cell uptake of these nanoparticles. These data are further in line with the absence of luciferase expression (*vide supra*).

By contrast, and as illustrated in Fig. 12(A), a clear increase of fluorescence intensity associated to the folate overexpressing KB(+) cells was observed when these cells were incubated with the YOYO-labeled and targeted [N-F4C10CysTEGNH3]$_2$/DNA N/P 4 nanoparticles. This fluorescence increase was further significantly more important than that observed for the KB(+) cells incubated with the complexes lacking the folic acid ligand, and also more important than that for the control KB(−) cells incubated with the targeted ones (Fig. 12(B)). Moreover, competition experiments in the presence of folic acid in excess decreased the fluorescence associated to the KB(+) cells incubated with the targeted nanoparticles (Fig. 12(A)) to a level comparable to that measured for the untreated KB(+) cells. The biparametric analysis of the flow cytometry data (Fig. 13) confirmed further that (i) at least 70% of the cells took up, similar, yet moderate amounts of the fluorescent targeted complexes (Fig. 13(A)), and (ii) the presence of excess folic acid inhibited almost completely the uptake of these targeted complexes (only 2% of fluorescent-positive cells; Fig. 13(B)). Moreover, only 7% of fluorescent-positive cells only were observed when the KB(+) cells were incubated with the complexes lacking the folic acid ligand (Fig. 13(C)). Altogether, these experiments indicate clearly a specific cellular uptake of the folic-acid targeted DNA nanoparticles by the KB(+) cells as a result of specific interactions between the folic acid conjugate and the folic acid receptor expressed by the KB(+) cells. These specific interactions led further to a more

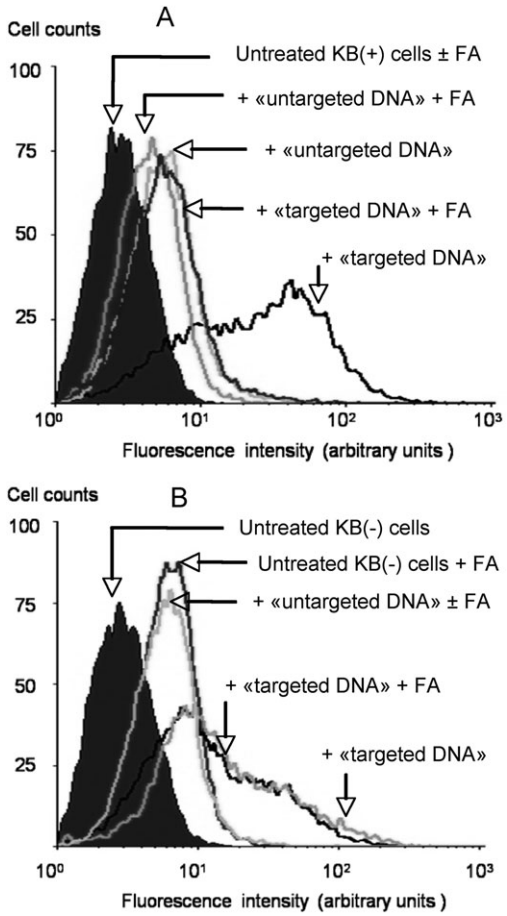

Fig. 12 Flow cytometry of (A) folate over-expressing KB(+) cells, and (B) KB(−) cells exposed for 4 h to uncoated or 5 mol% [N-F6C10CysPEG-FA]$_2$-coated [N-F4C10CysTEGNH3]$_2$/YOYO-DNA (= pTG11236) nanoparticles at a DNA concentration of 15 μM phosphate, in the absence or presence of 1 mM folic acid (FA). For more details, see Experimental section.

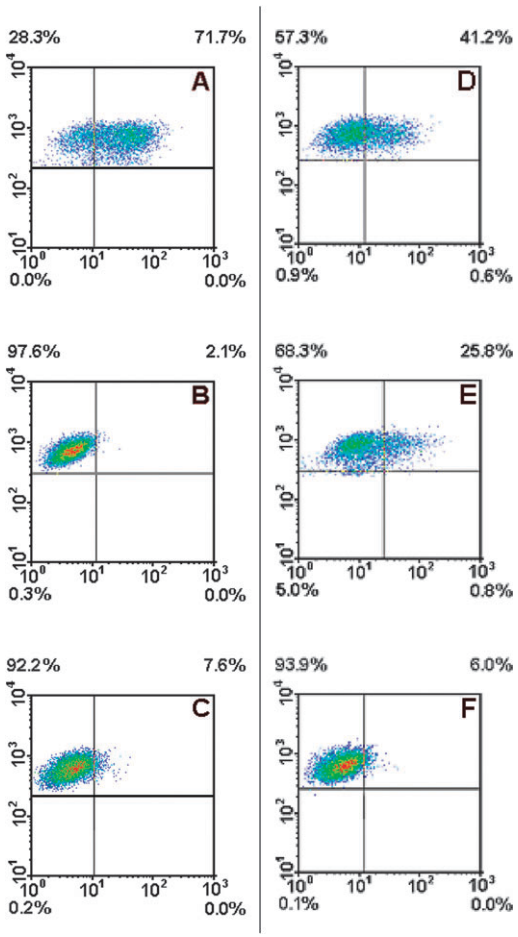

Fig. 13 Biparametric cytograms (density plot) of KB(+) cells (panels A–C) and KB(−) cells (panels D–F) exposed for 4 h to uncoated (panels C, F) or 5 mol% [N-F6C10CysPEG-FA]$_2$-coated [N-F4C10CysTEGNH3]$_2$/YOYO-DNA(= pTG11236) nanoparticles at a DNA concentration of 15 μM phosphate, in the absence (panels A, D) or presence of 1 mM folic acid (FA) (panels C, F). x axis represents YOYO marking, y axis represents front scattering intensity. Percentage of residual fluorescence in each zone is indicated on each corner. Left upper zone: autofluorescence of cells; right upper zone: YOYO-positive cells.

important cellular uptake than that resulting from non-specific interactions.

Concerning the control experiments performed with the KB(−) cells (Fig. 12(B) and 13(D)–(F)), it should be emphasized that (i) the cellular uptake of the targeted complexes was significantly more important than for the non-targeted ones (nearly 42% *vs.* 6% of fluorescent-positive cells; Fig. 13(D) and (F)), and (ii) the competition with free folic acid induced only 40% of cellular uptake inhibition of the targeted complexes (26% of fluorescent-positive cells; Fig. 13(E)). These results indicate that the KB(–) cells (which do express to some extent the folic acid receptors) took up the targeted complexes through both a specific folic acid-receptor mediated and unspecific heparan sulfate proteoglycan-mediated mechanism.

Surprisingly, if flow cytometry showed a cellular uptake significantly more important for the targeted complexes than for the untargeted ones, our transfection luciferase assays indicated however the opposite sequence. Unsuccessful transfection increase with the folic acid-targeted formulations may thus likely arise from their uptake and subsequent storage into intracellular compartments (such as caveolae) from which they cannot escape. Indeed, caveolae were thought to be folic acid-storing organelles and vehicles for transcytosis,[51] a function being nonproductive for gene delivery and expression.

Conclusions

A novel and straightforward synthesis (three steps with 45–50% overall yields) of dimerizable perfluoroalkylated thiol detergents deriving from cysteine and containing a monocationic aminotriethylene glycol or a tricationic linear spermine polar head was performed. These derivatives were successfully used to condense DNA into a monodisperse population of negatively or positively charged [F-detergent]$_2$/DNA nanoparticles, as confirmed by zeta potential and agarose gel electrophoresis experiments. These stable, virus-sized (~40–80 nm) nanoparticles consisted likely into monomolecular DNA particles though particles containing a few copies of DNA could not be excluded. These constructs were obtained following a monomolecular DNA condensation process occurring when DNA is mixed with a cationic detergent at a concentration close to its CMC, the resulting complexes being subsequently stabilized upon oxidation of the thiol detergent into its disulfide [F-detergent]$_2$ lipid on the DNA matrix. DNA was also shown to be fully protected, not accessible, when condensed into cationic nanoparticles. The surface of these particles was further successfully labeled with an amphiphilic-PEG–folic acid conjugate, as attested by zeta potential measurements. Size measurements and TEM analysis showed nanometric sizes ($\leq$80 nm) for these labeled [F-detergent]$_2$/DNA nanoparticles.

Noticeably with respect to their very low size, we found that the cationic, uncoated [F-detergent]$_2$/DNA formulations were efficient ''non-specific'' transfection agents of KB cells and particularly more efficient than PEI polyplexes. However, though FACS analysis with (un)coated and YOYO-labeled [F-detergent]$_2$/DNA nanoparticles showed specific uptake of the folic acid coated nanoparticles into folate-overexpressing KB cells, transfection experiments relying on luciferase expression measurements did not show any specific improvement of gene expression resulting from such a targeting. Further experiments are needed to acquire more information about the cell uptake, intracellular localization and trafficking of the internalized nanoparticles (endosomal release, intracellular *vs.* nuclear localization, *etc.*).

Acknowledgements

We thank the ''Région Provence-Alpes-Côte d'Azur'' and the CNRS for a grant (L. L.). We would particularly like to thank the ''Laboratoire de Physique de la Matière Condensée (UMR 6622 CNRS Université de Nice Sophia-Antipolis) as well as the ''Laboratoire Immunité anti-tumorale et chimiotactisme'' (INSERM U638, Université de Nice Sophia-Antipolis) for their help in PALS and flow cytometry experiments, respectively.

References

1 B. Demeneix, Z. Hassani and J.-P. Behr, *Curr. Gene Ther.*, 2004, **4**, 445–455.
2 E. Wagner, *Pharm. Res.*, 2004, **21**, 8–14.
3 B. Martin, M. Sainlos, A. Aissaoui, N. Oudrhiri, M. Hauchecorne, J. P. Vigneron, J. M. Lehn and P. Lehn, *Curr. Pharm. Des.*, 2005, **11**, 375–394.
4 E. Mastrobattista, S. A. Bravo, M. van der Aa and D. J. A. Crommelin, *Drug Discovery Today: Technol.*, 2005, **2**, 103–110.
5 E. Mastrobattista, M. A. E. M. van der Aa, W. E. Hennink and D. J. A. Crommelin, *Nat. Rev. Drug Discovery*, 2006, **5**, 115–121.
6 S. Jin and K. M. Ye, *Biotechnol. Prog.*, 2007, **23**, 32–41.
7 A. Aissaoui, N. Oudrhiri, L. Petit, M. Hauchecorne, E. Kan, M. Sainlos, S. Julia, J. Navarro, J.-P. Vigneron, J.-M. Lehn and P. Lehn, *Curr. Drug Targets*, 2002, **3**, 1–16.
8 E. Wisse, R. B. De Zanger, K. Charels, P. Van Der Smissen and R. S. McCuskey, *Hepatology*, 1985, **5**, 683–692.
9 N. N. Sanders, S. C. De Smedt, E. Van Rompaey, P. Simoens, F. De Baets and J. Demeester, *Am. J. Respir. Crit. Care Med.*, 2000, **162**, 1905–1911.
10 S. S. Olmsted, J. L. Padgett, A. I. Yudin, K. J. Whaley, T. R. Moench and R. A. Cone, *Biophys. J.*, 2001, **81**, 1930–1937.
11 C. M. Feldherr and D. Akin, *J. Cell Biol.*, 1991, **115**, 933–939.
12 G. L. Lukacs, P. Haggie, O. Seksek, D. Lechardeur, N. Freedman and A. S. Verkman, *J. Biol. Chem.*, 2000, **275**, 1625–1629.
13 K. Ribbeck and D. Gorlich, *EMBO J.*, 2001, **20**, 1320–1330.
14 V. Kolb-Bachofen, J. Schlepper-Schaefer and H. Kolb, *Exp. Cell Res.*, 1983, **148**, 173–182.
15 M. K. Bijsterbosch, G. J. Ziere and T. J. C. Van Berkel, *Mol. Pharmacol.*, 1989, **36**, 484–489.
16 J. A. Reddy and P. S. Low, *Crit. Rev. Ther. Drug Carrier Syst.*, 1998, **15**, 587–627.
17 T. Blessing, J.-S. Remy and J.-P. Behr, *Proc. Natl. Acad. Sci. USA*, 1998, **95**, 1427–1431.
18 E. Dauty, J.-S. Remy, T. Blessing and J.-P. Behr, *J. Am. Chem. Soc.*, 2001, **123**, 9227–9234.
19 E. Dauty, J.-S. Remy, G. Zuber and J.-P. Behr, *Bioconjugate Chem.*, 2002, **13**, 831–839.
20 M. Ouyang, J.-S. Remy and F. C. Szoka, Jr, *Bioconjugate Chem.*, 2000, **11**, 104–112.
21 J. P. Behr, *Tetrahedron Lett.*, 1986, **27**, 5861–5864.
22 S. M. Mel'nikov, V. G. Sergeyev and K. Yoshikawa, *J. Am. Chem. Soc.*, 1995, **117**, 2401–2408.
23 K. Fabio, C. Di Giorgio and P. Vierling, *Biochim. Biophys. Acta*, 2005, **1724**, 203–214.
24 J. G. Riess, F. Frezard, J. Greiner, M. P. Krafft, C. Santaella, P. Vierling and L. Zarif, Membranes vesicles and other supramolecular systems made from fluorinated amphiphiles, , in *Handbook of Nonmedical Applications of Liposomes*, ed. D. D. Lasic and Y. Barenholz, CRC, Boca Raton FL, 1996, vol. 3, pp. 97–141.

25 P. Vierling, C. Santaella and J. Greiner, *J. Fluorine Chem.*, 2001, **107**, 337–354.
26 J. Gaucheron, C. Santaella and P. Vierling, *Bioconjugate Chem.*, 2001, **12**, 114–128.
27 O. Boussif, J. Gaucheron, C. Boulanger, C. Santaella, H. V. Kolbe and P. Vierling, *J. Gene Med.*, 2001, **3**, 109–114.
28 L. Le Gourrierec, C. Di Giorgio, J. Greiner and P. Vierling, *Tetrahedron*, 2008, **64**, 2233–2240.
29 R. J. Lee and L. Huang, *J. Biol. Chem.*, 1996, **271**, 8481–8487.
30 J. A. Reddy and P. S. Low, *J. Controlled Release*, 2000, **64**, 27–37.
31 J. A. Reddy, D. Dean, M. D. Kennedy and P. S. Low, *J. Pharm. Sci.*, 1999, **88**, 1112–1118.
32 C. P. Leamon and P. S. Low, *Drug Discovery Today*, 2001, **6**, 44–51.
33 C. P. Leamon, I. Pastan and P. S. Low, *J. Biol. Chem.*, 1993, **268**, 24847–24854.
34 L. R. Coney, A. Tomassetti, L. Carayannopoulos, V. Frasca, B. A. Kamen, M. I. Colnaghi and V. R. Zurawski, Jr, *Cancer Res.*, 1991, **51**, 6125–6132.
35 I. G. Campbell, T. A. Jones, W. D. Foulkes and J. Trowsdale, *Cancer Res.*, 1991, **51**, 5329–5338.
36 L. T. Mantovani, S. Miotti, S. Menard, S. Canevari, F. Raspagliesi, C. Bottini, F. Bottero and M. I. Colnaghi, *Eur. J. Cancer*, 1994, **30A**, 363–369.
37 S. D. Weitman, R. H. Lark, L. R. Coney, D. W. Fort, V. Frasca, V. R. Zurawski, Jr and B. A. Kamen, *Cancer Res.*, 1992, **52**, 3396–3401.
38 W. A. Franklin, M. Waintrub, D. Edwards, K. Christensen, P. Prendegrast, J. Woods, P. A. Bunn and J. F. Kolhouse, *Int. J. Cancer. Suppl.*, 1994, **8**, 89–95.
39 N. O. Brace, *J. Org. Chem.*, 1962, **27**, 4491–4498.
40 D. S. Kemp and R. I. Carey, *J. Org. Chem.*, 1989, **54**, 3640–3646.
41 A. J. Geall and I. S. Blagbrough, *Tetrahedron*, 2000, **56**, 2449–2460.
42 A. Chattopadhyay and E. London, *Anal. Biochem.*, 1984, **139**, 408–412.
43 K. Sou, T. Endo, S. Takeoka and E. Tsuchida, *Bioconjugate Chem.*, 2000, **11**, 372–379.
44 C. J. Wheeler, P. L. Felgner, Y. J. Tsai, J. Marshall, L. Sukhu, S. G. Doh, J. Hartikka, J. Nietupski, M. Manthorpe, M. Nichols, M. Plewe, X. Liang, J. Norman, A. Smith and S. H. Cheng, *Proc. Natl. Acad. Sci. USA*, 1996, **93**, 11454–11459.
45 C. P. Leamon and P. S. Low, *Proc. Natl. Acad. Sci. USA*, 1991, **88**, 5572–5576.
46 J. P. Flinn, R. Murphy, J. H. Boublik, M. J. Lew, C. E. Wright and J. A. Angus, *J. Pept. Sci.*, 1995, **1**, 379–384.
47 V. A. Bloomfield, D. M. Crothers and I. Tinoco, Jr, in *Nucleic Acids: Structures Properties, and Functions*, University Sciences Book, Sausalito California USA, 2000, ch. 11 (pp. 475–534) and ch. 414 (pp. 725–773).
48 C. Chittimalla, L. Zammut-Italiano, G. Zuber and J. P. Behr, *J. Am. Chem. Soc.*, 2005, **127**, 11436–11441.
49 C. M. Wiethoff, J. G. Smith, G. S. Koe and C. R. Middaugh, *J. Biol. Chem.*, 2001, **276**, 32806–32813.
50 M. Belting, *Trends Biochem. Sci.*, 2003, **28**, 145–151.
51 M. Gumbleton, *Adv. Drug Delivery Rev.*, 2001, **49**, 281–300.

